Made available by Hasselt University Library in https://documentserver.uhasselt.be

Photo-induced copper-mediated (meth) acrylate polymerization towards graphene oxide and reduced graphene oxide modification

Peer-reviewed author version

RAILIAN, Svitlana; HAVEN, Joris; MAES, Lowie; DE SLOOVERE, Dries; Trouillet, V; Welle, A; ADRIAENSENS, Peter; VAN BAEL, Marlies; HARDY, An; DEFERME, Wim & JUNKERS, Tanja (2020) Photo-induced copper-mediated (meth) acrylate polymerization towards graphene oxide and reduced graphene oxide modification.
In: EUROPEAN POLYMER JOURNAL, 134 (Art N° 109810).

DOI: 10.1016/j.eurpolymj.2020.109810
Handle: http://hdl.handle.net/1942/33203

Photo-Induced Copper-Mediated (Meth)Acrylate Polymerization towards Graphene Oxide and Reduced Graphene Oxide Modification

Svitlana Railian,[1] Joris J. Haven,[2] Lowie Maes,[1] Dries De Sloovere,[3, 4, 5] Vanessa Trouillet,[6, 7] Alexander Welle,[7, 8] Peter Adriaensens,[5, 9] Marlies K. Van Bael,[3, 4, 5] An Hardy,[3, 4, 5] Wim Deferme[5, 10] and Tanja Junkers[1, 2*]

[1] Polymer Reaction Design group, UHasselt – Institute for Materials Research, Agoralaan, 3590 Diepenbeek, Belgium.

[2] School of Chemistry, Monash University, 19 Rainforest Walk, Clayton VIC 3800, Australia

[3] UHasselt – Institute for Materials Research, Inorganic and Physical Chemistry, Agoralaan, 3590 Diepenbeek, Belgium.

[4] Energyville, Thor Park 8320, B-3600 Genk, Belgium

[5] IMEC vzw – Division IMOMEC, Wetenschapspark 1, 3590 Diepenbeek, Belgium

[6] Institute for Applied Materials (IAM), Karlsruhe Institute of Technology (KIT), Hermann-von-Helmholtz-Platz 1, 76344 Eggenstein-Leopoldshafen, Germany

[7] Karlsruhe Nano Micro Facility (KNMF), Karlsruhe Institute of Technology (KIT), Hermann-von-Helmholtz-Platz 1, 76344 Eggenstein-Leopoldshafen, Germany

[8] Institute of Functional Interfaces, Karlsruhe Institute of Technology (KIT), Hermann-von-Helmholtz-Platz 1, 76344 Eggenstein-Leopoldshafen, Germany

[9] UHasselt – Institute for Materials Research, Nuclear Magnetic Resonance Spectroscopy Group, Agoralaan, 3590 Diepenbeek, Belgium.

[10] UHasselt – Institute for Materials Research, Wetenschapspark 1, 3590 Diepenbeek, Belgium.

* Corresponding Author: Tanja Junkers, Email: tanja.junkers@uhasselt.be, Homepage: www.polymatter.net, Twitter: @prd_group

Abstract

The preparation of well-dispersed graphene/polymer nanocomposites is challenging due to the poor miscibility of graphene sheets in a polymer matrix. To enhance the interaction between both phases, graphene sheets can be decorated with polymer chains. Herein, different strategies to graft poly(methyl methacrylate) (PMMA) and poly(di(ethylene glycol) ethyl ether acrylate) (PDEGA) chains at various positions on graphene oxide and reduced graphene oxide (GO/rGO) sheets are compared. Chain attachment was achieved by "grafting-to" and "grafting-from" methods. *Grafting-to* was performed by classical copper (I)-catalyzed alkyne azide cycloaddition. Using a *grafting-from* approach, PMMA and PDEGA brushes were grown from GO and rGO sheets *via* surface-initiated photo-induced copper-mediated polymerization (SI-photoCMP). SI-photoCMP is a robust and efficient method that allows polymerizations to be carried out under mild conditions and with reduced catalyst concentration. Moreover, the successful implementation of SI-photoCMP in a continuous-flow set-up enables easy upscaling of the system and is, therefore, a more efficient and environmentally friendly process for GO/rGO surface modification. By using the *grafting-to* approach, the grafting density of PMMA (M_n = 2,600 g/mol) was one chain per 990 carbons of graphene. In contrast, longer PMMA chains (M_n = 40,300 g/mol) and higher grafting density were obtained *via* the *grafting-from* method (one PMMA chain per 140 carbons of graphene).

Introduction

The synthesis of novel materials with tailor-made properties is essential in a variety of applications. Polymers are widely used materials. Their variety, processability, inherent mechanical properties, and light weight are highly attractive for designing new types of materials. In order to achieve tailored properties, polymers can be either molecularly modified, or be blended with another material that introduce properties that the polymer itself is lacking. Blended nanoparticles (nanofiller) in a polymer matrix, also referred to as nanocomposites, are hereby a very interesting approach.[1] One potential nanofiller that introduces sophisticated properties is graphene. Graphene has rapidly gained the attention of the scientific and industrial world after its relatively recent discovery in 2004.[2] Its unique combination of excellent electrical, thermal, optical, and mechanical properties makes it a highly suitable material to tailor polymer nanocomposites properties.[3] The performance of polymer/graphene nanocomposites depends significantly on the dispersion of the graphene sheets in the polymer matrix. Due to Van der Waals and π-π interactions, graphene sheets tend to agglomerate and phase separate on a micro- and nanoscale level leading to a reduced performance of the composite. Therefore, the pre-modification of graphene sheets with polymer chains is investigated to enhance the polymer/graphene miscibility. The use of graphene through bottom-up approaches is not preferred for polymer nanocomposite applications due to the high processing costs and small production scale.[3] Therefore, the focus switched to graphene oxide (GO) and reduced graphene oxide (rGO). This is mainly because of their better availability and more simple chemical functionalization. GO has a large quantity of oxygen-containing groups, such as hydroxyl and epoxy moieties, mainly situated on the basal plane of the GO sheets and carboxyl group located at the sheet edges.[4] The presence of such groups breaks, however, the aromatic structure of the sheets making GO electrically insulating.

The reduction of GO by chemical, thermal or ultraviolet-assisted methods allows to produce electrically conducting rGO.[5]

The covalent modification of GO/rGO surfaces with small organic molecules is based on two approaches: (i) *via* oxygen-containing groups[6] and (ii) *via* sp^2 carbons from the graphene sheet.[7] Surface modification with polymers has been widely investigated.[4, 8] In this regard, two main synthesis approaches are generally used, "grafting-to" and "grafting-from". The first is based on coupling pre-synthesized polymer chains to the GO surface *via* efficient conjugation chemistry, whereas the latter directly grows polymers from the surface after functionalization with a suitable initiator.[4, 8a, 8b] In the *grafting-to* approach, multiple synthesis routes are used for polymer conjugation on the surface, such as esterification,[9] amidation,[10] azide-alkyne cycloaddition,[11] nitrene cycloaddition,[12] condensation reactions[13] and radical coupling.[4, 14] The main advantage of this approach is the possibility to tailor and characterize the polymers before grafting them onto the surface. However, due to steric factors, lower grafting densities are achieved and longer reaction times are required due to the slow self-diffusion of the polymers. In *grafting-from*, polymers can be analyzed after cleavage from the surface[15] *via* basic hydrolysis,[16] acid catalyzed transesterification,[17] photo-detachment[18] or an atomic force microscopy pull-off method.[19] With *grafting-from*, the steric effect is minimized due to the fixed position of the initiator molecule on the surface and fast monomer self-diffusion, resulting in higher grafting densities. Polymers can be grown from the surface *via* conventional radical or reversible deactivation radical polymerization (RDRP) techniques. In conventional radical polymerizations, bare GO sheets have been successfully used as a radical source via opening of epoxy rings on the surface leading to the reduction of GO into rGO decorated with polymers.[20] In RDRP, polymers with predetermined molecular weight and low dispersity can be targeted.[21] Four RDRP techniques are predominantly

used for GO/rGO modification: (i) single electron transfer living radical polymerization (SET-LRP), (ii) atom transfer radical polymerization (ATRP), (iii) reversible addition-fragmentation chain transfer polymerization (RAFT) and (iv) nitroxide-mediated polymerization (NMP).[4, 8] One of the first reports on controlled surface initiated (SI)-ATRP from rGO was investigated by the Nutt group where rGO was modified with 2-(4-aminophenyl)ethanol followed by the introduction of an initiator to the rGO surface.[17, 22] By varying the concentration of styrene (St) monomer and the attached acrylic ATRP initiator on the surface, control over grafting densities and polymer chain length could be achieved. However, SI-ATRP could only be performed at higher temperatures (110 °C in the above-mentioned case of St) to initiate the polymerization reaction. Furthermore, long reaction times (10-24 hours) and high CuBr/PMDETA (*N,N,N',N'',N*''-pentamethyl-di-ethylenetriamine) concentrations were applied. Lower temperatures (65 °C) can be used to graft MMA chains using SI-ATRP.[23] Lee *et al.* used SET-LRP to grow St, MMA and butyl acrylate polymers from GO at 80 °C.[24]

Photo-induced RDRP routes have been progressively investigated for the synthesis of polymers under mild reaction conditions, mainly due to the development of highly efficient light sources (such as lasers, fluorescent lights, light emitting diodes) and the obvious environmental benefits.[25] Furthermore, photo-induced reactions are highly interesting due to the simple procedure, temporal control, and comparatively simple scalability. However, until now only little research has been performed on photo-induced surface-initiated polymerization on nanoparticles. UV-induced SI polymerization has been reported on TiO_2 nanoparticles.[26] Also, UV-induced SI-ATRP was used to grow polymer brushes from silica nanoparticles[27] and TiO_2-initiator nanowires.[28] In another approach, visible light-induced SI-ATRP was used to grow polymer brushes from TiO_2/rGO nanocomposites.[29]

The implementation of flow chemistry for photo-induced SI polymerization has many advantages such as improved safety, high reproducibility, fast heat exchange, easy scalability, operation above ambient pressure boiling points of reactants and – most importantly – improved homogeneous irradiation by light sources as was previously demonstrated.[30] Continuous flow synthesis is widely implemented in organic chemistry,[31] and is also in polymer chemistry becoming more and more a routine technique for improving control over polymerizations. Generally, better control over polymer length and dispersity is achieved by using flow reactors.[32] The first combination of photo-induced copper-mediated polymerization (photoCMP)[33] and continuous flow reactors was described by Junkers and coworkers.[30c, 34] photoCMP is typically applied under UV irradiation, but also visible light can be employed with the correct choice of catalyst and ligand.[35] Moreover, a number of carbon-based materials was used for surface functionalization in continuous-flow reactors such as fullerenes,[36] carbon nanotubes[37] and rGO.[38] Combination of the two approaches appears to be highly rewarding, also form the aspect of scalability of GO modifications.

In this manuscript we investigate different strategies to graft polymer brushes at different positions to graphene oxide and reduced graphene oxide (GO/rGO) sheets, on either the basal plane, sheet edges or both. To influence the dispersibility of graphene-based sheets in a variety of solvents and polymer matrices, two acrylic monomers were selected for grafting: (i) the hydrophobic monomer methyl methacrylate (MMA), and (ii) the more hydrophilic di(ethylene glycol) ethyl ether acrylate (DEGA). For the first time, the implementation of photoCMP as a *grafting-from* procedure to grow polymer brushes from three graphene-based surfaces (GO, *in situ* formed rGO and commercially available rGO) was investigated. Polymerization reactions were performed under UV light in the presence of a copper catalyst. Copper can be disadvantageous in some biomedical applications and

hence, the minimum copper concentration necessary for efficient polymer grafting was also explored. Next, a comparative study of traditional batch and flow set-up on surface grafting *via* photoCMP was performed. Flow reactors allow for scalability of polymerization reactions, a well-known challenge to overcome in UV-induced batch polymerizations. Coupling of PMMA and PDEGA to the GO surface was explored *via* the *grafting-to* approach using classical copper (I)-catalyzed alkyne azide cycloaddition (CuAAC). Furthermore, grafting densities were compared for both approaches.

Results and Discussion

Modification of GO/rGO surfaces.

Graphene-based sheets were grafted with PMMA (hydrophobic) and PDEGA (hydrophilic) to enhance the miscibility in a compatible polymer matrix. The grafted polymer chains prevent aggregation of the sheets by improving the interfacial interaction with the polymer matrix. In this manner, good dispersion can be achieved and the obtained grafted materials can be directly used as a filler in polymer nanocomposites. Four grafting strategies were applied to graft polymers brushes on GO and rGO surfaces, including one *grafting-to* (*via* CuAAC) and three *grafting-from* (*via* SI-photoCMP) approaches as illustrated in Scheme 1. Grafting densities, grafting positions on the graphene sheets (basal plane, sheet edges, or both) and polymer molecular weight (distributions) were studied. In the CuAAC and SI-photoCMP/1 methods (Scheme 1), the polymer chains were grafted on the sheet edges (CuAAC) and the basal plane (SI-photoCMP/1) of GO by the use of the large quantity of oxygen-containing groups present on the surface. However, subsequent chemical or thermal treatment is required to recover the aromatic structure of the GO

sheets in order to restore its thermal and electrical properties.[3] In SI-photoCMP/2 (Scheme 1), post-treatment was avoided *via in situ* thermal reduction and formation of rGO prior to the polymerization step. Reduction of GO to rGO was achieved at elevated temperature of modification of carboxyl functional groups with ethylene glycol. *Via* this route, polymers can be grafted from both sheet edges and the basal plane. Thus, a high concentration of functional groups on the surface and efficient coupling of ethylene glycol is required to obtain high grafting densities. To overcome this potential limitation of SI-photoCMP/2, another approach was introduced. In SI-photoCMP/3, the modification of commercially available rGO was performed by using the double bond functionalities of the sheets *via* a diazotization reaction. SI-photoCMP/3 allows grafting the polymers at the sheet edges and the basal plane.

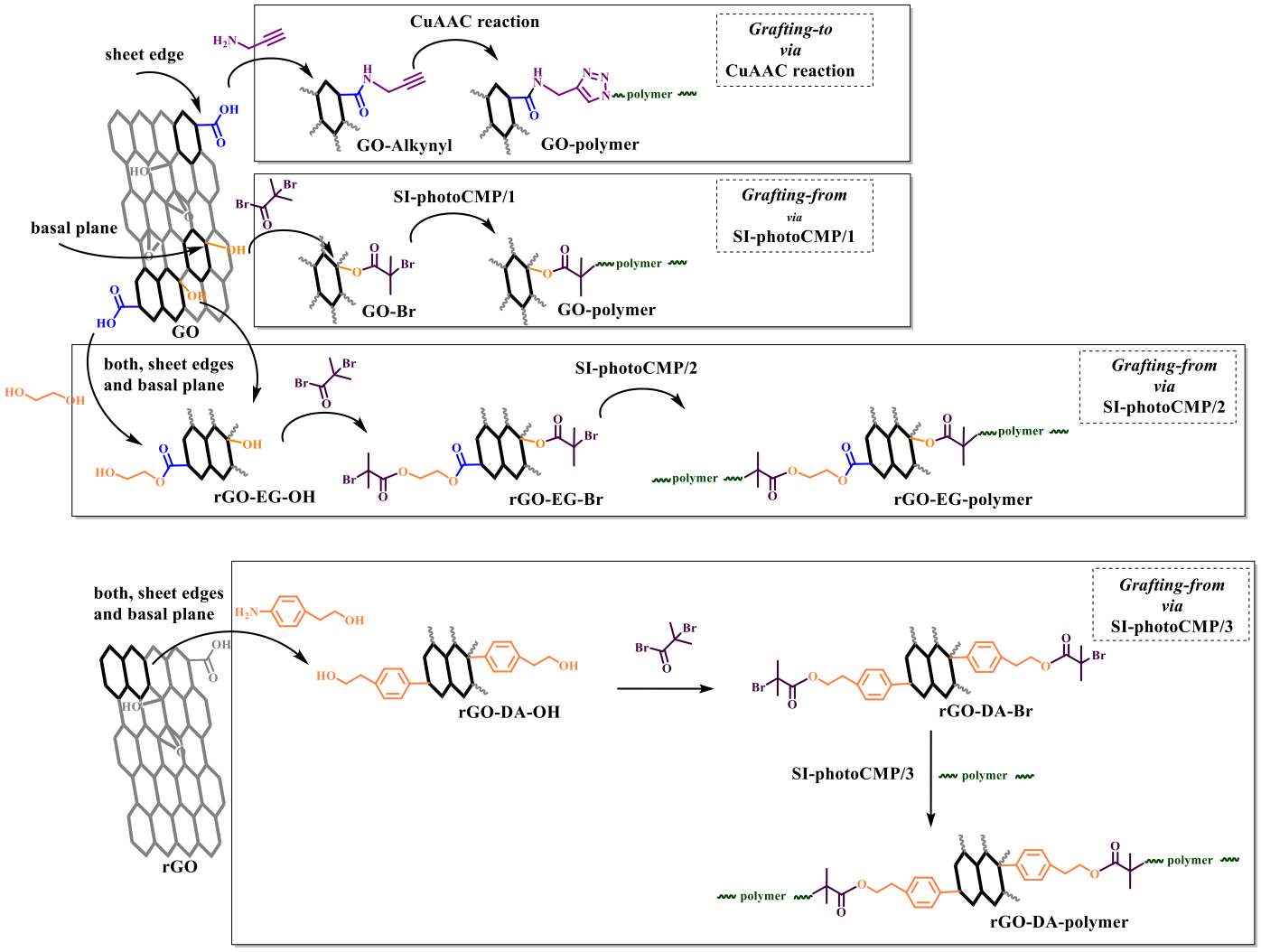

Scheme 1. General synthesis scheme of GO/rGO surface modifications.

"Grafting-to" approach for PMMA and PDEGA attachment to GO.

Grafting-to comprises a two-step procedure where first alkynyl groups are attached to the GO surface, followed by CuAAC to graft the polymer chains (Scheme S1). Modification strategies have been investigated to graft a variety of azide-terminated polymer chains, such as poly(styrene) (PSt),[11] poly(*N*-isopropyl acrylamide) (PNIPAM)[39] and poly(ethylene glycol) (PEG).[40]

Herein, to compare the influences of molecular weight on grafting, PMMA and PDEGA with different molecular weight were synthesized *via* photoCMP.[41] Four polymers were obtained and modified with azide (N_3) endgroup functionality. PMMA-N_3 (M_n = 2,600 g/mol and M_n = 7,100 g/mol) and PDEGA-N_3 (M_n = 2,700 g/mol and M_n = 8,000 g/mol) were obtained with dispersities ($Đ$) < 1.34 as analyzed *via* size-exclusion chromatography (SEC, Figure 1). The GO surface was modified *via* an amidation reaction between the carboxyl groups of GO and amino groups of propargyl amine yielding alkyne functionalities on the surface (GO-Alkynyl, Scheme S1).[39] The GO-Alkynyl surface was analyzed *via* Fourier-transform infrared spectroscopy (FT-IR), X-ray photoelectron spectroscopy (XPS) and solid-state ^{13}C nuclear magnetic resonance (solid-state ^{13}C NMR) to verify the successful modification (see supporting information for details). Subsequently, the CuAAC reaction was performed to graft various polymers to the GO-Alkynyl sheet surface with CuBr/PMDETA as the catalyst system in dimethylformamide (DMF) (Table S3).[11, 39] As described before, the CuAAC approach only allows grafting to the sheet edges of GO where carboxyl groups are present (Scheme S1).

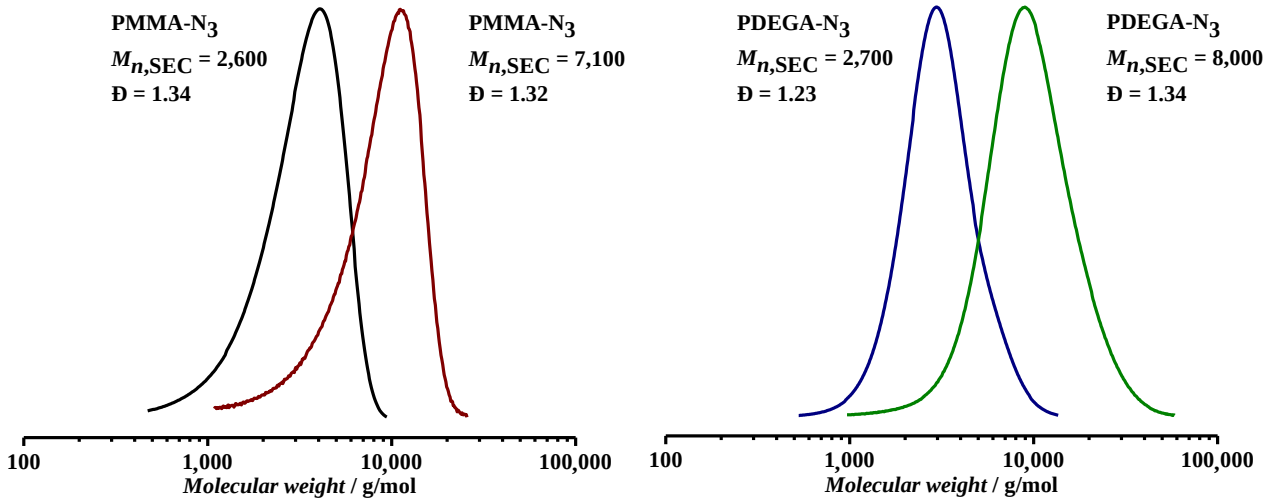

Figure 1. SEC traces of PMMA and PDEGA used for *grafting-to* modification of GO-Alkynyl surface.

Thermogravimetric analysis (TGA) is a widely used technique to assess the success of polymer grafting (*i.e.* the amount of grafted polymer in wt%) or grafting density on a surface by determining the mass loss during heating on a surface by determining the mass loss during heating.[42] Grafting density is the number of bound polymers per unit surface area (*e.g.* per nm^2 or per # carbons of graphene).[43] Figure 2 shows the thermogravimetric profiles for the GO grafted with PMMA and PDEGA as previously described. The degree of polymer grafting was determined from the difference in weight loss between GO-Alkynyl and GO-PMMA or GO-PDEGA at 600 °C. Such temperature (600 °C) was chosen as a point where polymers underwent thermal degradation and before substantial degradation of graphene plane. A higher polymer grafting was observed for the hydrophilic PDEGA (M_n = 2,700 g/mol, 18.7 wt% grafted to GO-Alkynyl), compared to PMMA (M_n = 2,600 g/mol, 9.4 wt% grafted to GO-Alkynyl) which could be explained by the better solubility of PDEGA in DMF.[44] In a poor solvent the surface-grafted polymer is more likely to have a mushroom structure[45] that lowers the grafting density due to steric hindrince. Based on the

TGA results, higher grafting was achieved for shorter polymer chains possibly due to the lower diffusivity and increased steric hindrince for longer polymer chains.[46] The grafting efficiencies described here are in-line with previously reported grafting of PSt (20% with M_n = 4,600 g/mol)[11] and PNIPAM (50% with M_n = 3,800 g/mol) using CuAAC coupling.[39]

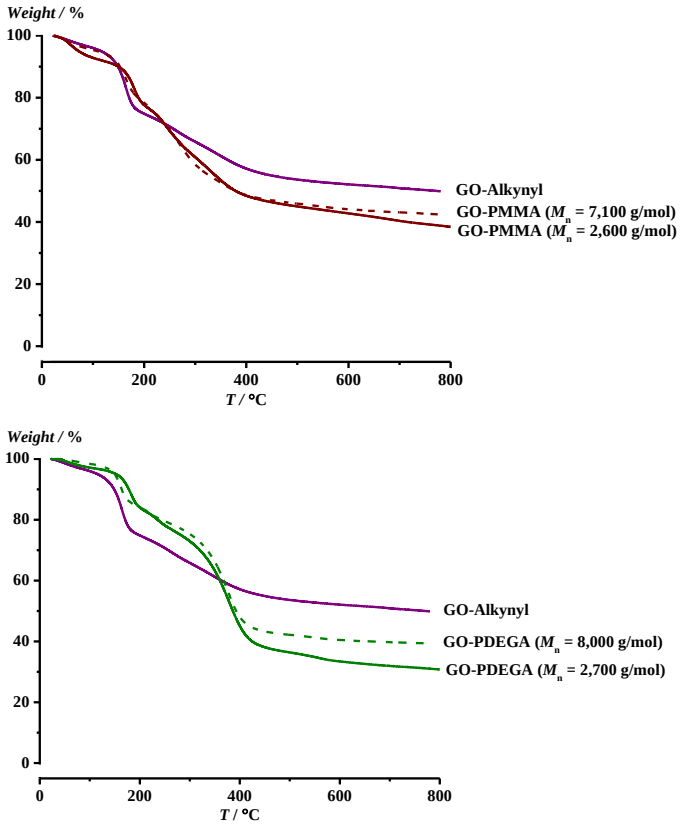

Figure 2. TGA thermograms of surface-functionalized GO-PMMA and GO-PDEGA *via* CuAAC conjugation (*grafting-to* approach).

"Grafting-from" approach for PMMA and PDEGA growth from GO, *in situ* formed rGO and commercial rGO.

In **SI-photoCMP/1**, the GO surface was modified with a suitable ATRP initiator (see Scheme S2). An esterification reaction was performed between the hydroxyl groups of GO and acyl bromide

groups of 2-bromoisobutyryl bromide resulting in GO-Br.[47] XPS measurements confirmed the successful surface modification *via* the detection of Br $3d_{5/2}$ at 70.1 eV, proving the presence of covalently bound bromine with an atomic content of 0.3% (Table S1). Next, SI-photoCMP was carried out under UV-light (~365 nm). Polymers only grew from the basal plane of GO sheets due to the location of hydroxyl groups on the basal plane (Scheme S2).

In **SI-photoCMP/2**, the *in situ* fomation of rGO and subsequent polymer growth was investigated (Scheme S3). The presence of hydroxyl functionalities on GO surface is crucial for introducing an initiator. Additional hydroxyl groups were attached to the GO surface *via* the transformation of the existing carboxyl groups on the sheet edges into acid chlorides (*via* reaction with thionyl chloride) followed by direct quenching with ethylene glycol, followed by the *in situ* thermal reduction of the sheets (at 120 °C) and formation of rGO-EG-OH.[23] After introducing an initiator on the surface, the resulting rGO-EG-Br was used to grow polymers similar to SI-photoCMP/1. *Via* this route the polymer can be grafted from both the sheet edges and basal plane of rGO (Scheme S3).

All modification steps are equally of high importance to insure successful polymer grafting. FT-IR analysis of rGO-EG-OH shows the C-H (from $-CH_2-O-$ group) stretching mode vibration of the attached ethylene glycol at 2,926 cm^{-1} (Figure S1). After modification with a suitable initiator covalently bonded Br was detected in the rGO-EG-Br sample (2.2 atomic %), *via* XPS, compared to 0.3 atomic % in GO-Br as described in SI-photoCMP/1 (Table S1). Clearly, this modification strategy is yielding better results, explained by the higher reactivity of the primary -OH groups of ethylene glycols and lower reactivity of tertiary -OH, directly bonded to GO surface.

SI-photoCMP/3 (Scheme S4). To also test for the grafting of commercially available rGO, a further strategy was explored. RGO has fewer hydroxyl functionalities compared to GO, and thus

an additional reaction step needed to be performed to increase the abundance of -OH functionalities on the surface. This was achieved by the coupling of a hydroxyl-terminated molecule to the double bond functionalities of rGO. To do so, 2-(4-aminophenyl)ethanol was attached *via* a diazotization between the C(sp^2) of rGO and *in situ* generated diazonium species. The isoamyl nitrite was added to generate the diazonium salt to avoid storage of unstable and light-sensitive aryl diazonium salts.[22, 48] The resulting rGO-DA-OH sheets were further modified as above with ATRP-type initiator, forming rGO-DA-Br. Finally, also for this substrate SI-photoCMP was carried out resulting in polymers growth from both the sheet edges and basal plane of rGO (Scheme S4).

FT-IR analysis shows that rGO-DA-OH features the desired C-H (from -CH_2-O- group) stretching mode vibration of the attached 2-phenylethanol at 2,915 cm^{-1} (see Figure S1). A similar Br content was detected in rGO-DA-Br sample (2.2 atomic %), determined by XPS, compared to rGO-EG-Br. Attachment of phenethyl alcohol was also confirmed by solid-state ^{13}C NMR (appearance of the -CH_2 resonance at 32 ppm). Modification of the surface with the bromine suitable initiator was also indicated by NMR (peak at 172 ppm assigned to the R-C(O)-OR functionality, see Figure S2).

SI-photoCMP grafting reactions. As mentioned in the introduction, conventional ATRP was successfully applied to grow polymers from GO and rGO at elevated temperatures. By using SI-photoCMP, photons from a light source can generate radicals from photoinitiators at ambient temperature.[25b] First, SI-photoCMP was carried out under UV-light (~365 nm) in a conventional batch reactor for 24 hours. The batch reactor used for this purpose was a commercial UV nail gel curing lamp equipped with four 9 W bulbs (Figure 3). In a batch reactor light does not penetrate deep into the reaction mixture.[30c] In addition, GO is a relatively strong UV absorber. UV spectra of GO has a maximum absorption peak at 230 nm, attributed to $\pi \rightarrow \pi^*$ transitions of aromatic C=C bonds, thus in all UV-induced reactions, a fraction of the light is absorbed by GO.[49] As a

consequence, longer reaction times and vigorous stirring were required to perform SI-photoCMP in batch reactors. Conventional photo-batch reactors do not allow for reaction upscaling since the irradiation process is hindered by the light intensity gradient in the solution.

Thus, we also investigated photografting in continuous flow reactors.[30c] To this end, the same reaction conditions were used which then resulted in only 1 hour residence time (as faster reactions can be expected in continuous flow). The flow set-up was custom-build from gastight perfluoroalkoxy (PFA) tubing with 0.75 mm inner diameter wrapped around two UV-light bulbs (alternately in a figure-of-eight) and a syringe pump with a 20 mL syringe (Figure S6). Inside the syringe, six polytetrafluoroethylene-coated (PTFE-coated) octagonal stir bars (5 mm × 2 mm) were loaded to keep the GO-Initiator well dispersed.

SI-PhotoCMP of MMA from the GO-initiator surface was performed in the presence of a catalyst ($CuBr_2$) and ligand (PMDETA) with a mass ratio of [GO-Initiator] : [$CuBr_2$] : [PMDETA] = 1 : 0.34 : 0.85 in DMF/MeOH. To grow DEGA from the GO-Initiator surface, tris-(2-(dimethylamino)ethyl)amine (Me_6TREN) was used as a ligand with a mass ratio of [GO-Initiator] : [$CuBr_2$] : [Me_6TREN] = 1 : 0.24 : 1.5. The grafting of DEGA was possible in EtOH/H_2O mixtures as a greener solvent alternative. It has been reported before that SI-PhotoCMP can be carried out at extremely low catalyst concentration (0.137 μmol).[50] To graft MMA, the catalyst concentration has been reduced from 7.5 mmol to 1.88 mmol (4 times below standard protocol). For DEGA grafting, 10 times lower catalyst concentration was investigated: from 5.4 mmol to 0.54 mmol. These reactions are described in Table S4.

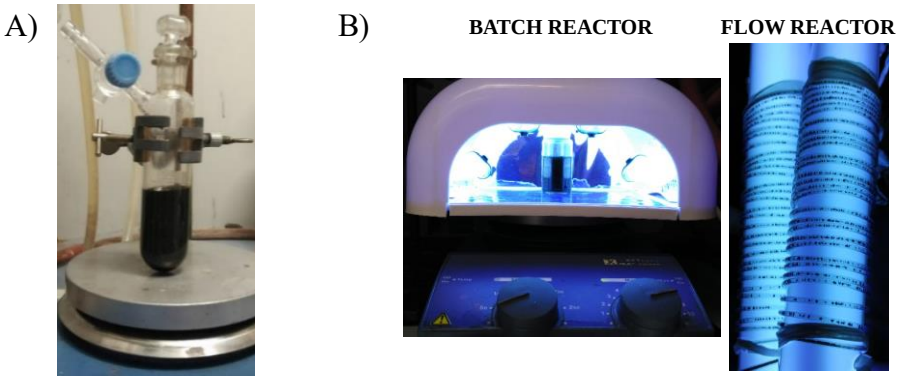

Figure 3. A) Batch reactor used for alkyne-azide cycloaddition. B) Batch and flow reactor set-ups used for SI-photoCMP.

Different from polymerization in solution, the information towards monomer conversion and the molecular weight is more difficult to obtain for surface-initiated polymerization. Instead, polymer grafting was calculated from TGA to estimate the success of SI-photoCMP at different reaction conditions. Additionally, control experiments were performed that followed the exact same synthesis procedure as for SI-photoCMP in absence of monomer to assess the influence of UV-induced GO reduction. Thus, GO-Br-blank, rGO-EG-Br-blank, and rGO-DA-Br-blank were synthesized. TGA shows the improved thermal stability of control (blank) samples, due to the partial removal of oxygen-content groups from the GO/rGO surface.

First, thermograms of samples prepared in batch reactors for 24 hours in the presence of catalyst (7.5 mmol for MMA grafting and 5.4 mmol for DEGA grafting) were investigated (Figure 4). The highest polymer content was obtained for samples prepared *via* the SI-photoCMP/3 method (60.1 wt% PMMA and 50.6 wt% PDEGA grafted to rGO-DA-Br, Table S6). The lowest polymer grafting was observed for the SI-photoCMP/1 approach (29.6 wt% PMMA and 23.5 wt% PDEGA grafted to GO-Br), presumably due to the comparatively low initiator concentration in these samples.

Next, 4 times (1.88 mmol for MMA grafting) and 10 times (0.54 mmol for DEGA grafting) lower catalyst concentration and ligand concentration were further investigated to minimize the amount of copper present in the residual composites. Compared to the above results, the thermograms showed for these cases reduced polymer grafting for all GO-Initiator systems (Figure S4), indicating the importance of sufficient catalyst concentration in reaction mixture.

The use of a continuous-flow reactor in photo-induced polymerizations results into better irradiation and fast polymerization of the reaction mixture.[41b, 51] Scale-up in flow reactors is typically achieved by using longer reactors or larger tubing diameters. SI-photoCMP was carried out in the continuous-flow reactor with inner tubing diameter 0.75 mm for 1 hour residence time (compared to 24 hours in batch). Longer residence times are typically not favoured in flow reactors in order to keep throughput in the reactor ideal. The thermograms show similar results for the flow products as for the batch reactions (Figure S5). Thus, a very significant improvement with respect to reaction time (>42.9 wt% polymer grafted to rGO-EG-Br and rGO-DA-Br, Table S6) is observed for SI-photoCMP/2 and SI-photoCMP/3 methods in flow compared to conventional SI-ATRP and SI SET-LRP where the typical range of 10-24 hours in batch needs to be applied.[8c, 22, 52]

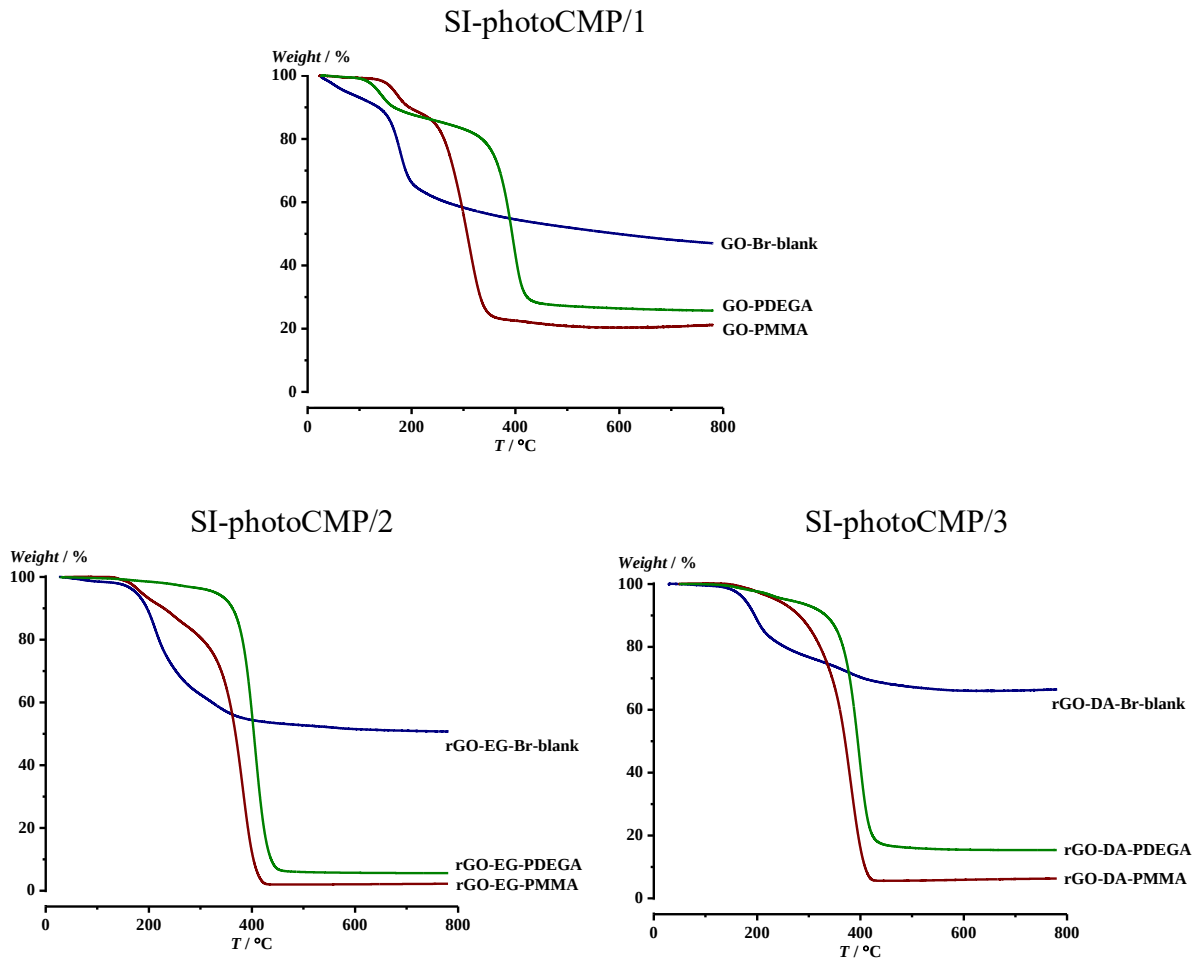

Figure 4. TGA thermograms of PMMA and PDEGA functionalized GO/rGO sheets *via* SI-photoCMP procedures. SI-PhotoCMP was carried out in UV-batch reactor at catalyst concentrations (5.4 mmol and 7.5 mmol).
The polymer-grafted samples are compared to relevant blank samples.

Figure 5 summarizes the obtained results for polymer grafting towards tested SI-photoCMP conditions (batch; flow and reduced catalyst concentration in batch reactors) based on TGA. Results are given as amount of polymer grafting (in grams) to 1 gram of graphene as this allows for a more meaningful comparison between different types of GO/rGO. This comprises the different oxidation level of GO/rGO surfaces and length of the spacer between surface and polymer chain.

In general, the lowest polymer grafting was observed using SI-photoCMP/1, compared to SI-photoCMP/2,3, due to the low concentration of attached initiator. Performing SI-photoCMP in a batch reactor results in the best grafting, compared to the flow reactor. The grafting reaction in flow reactor is highly efficient owing to the reaction time needed. Furthermore, performing SI-photoCMP in a batch reactor at lower catalyst concentration decreases the grafting efficiency. Polymerization of acrylates monomers in solution *via* photoCMP is more efficient compared to meth(acrylates).[41b, 51] A difference that typically needs to be taken into account for polymerizing methacrylates or acrylates via photoCMP is the choice of ligand. Methacrylates show better polymerization activity with PMDETA, while acrylates are polymerized more efficiently by using Me_6TREN.[40b] This difference, and the generally higher rate of polymerization for acrylates, should however, not be confused with a presumably lower grafting density. Grafting efficiency is given my more than mere speed of polymerization, but also by the choice of monomers, chain interactions, and lastly radical quenching by termination, which is significantly lower for methacrylates. With this consideration, it is yet an interesting observation that almost in all tested reaction conditions, higher grafting efficiencies were achieved for MMA compared to DEGA.

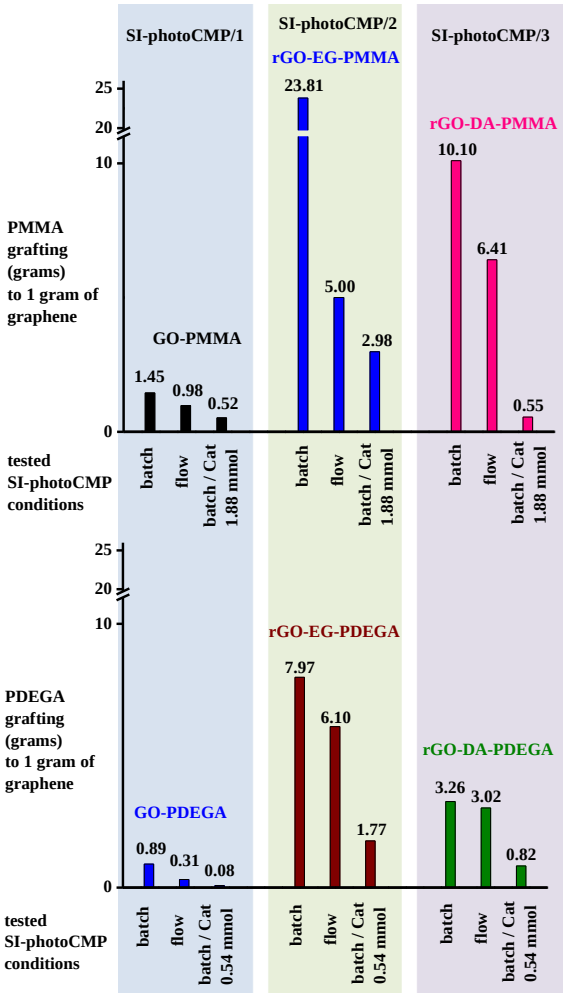

Figure 5. Comparison of PMMA and PDEGA grafting from GO/rGO sheets *via* SI-photoCMP procedures. SI-PhotoCMP was carried out in batch, flow and batch reactor at reduced catalyst concentration. Results are obtained from TGA.

Detailed investigation of polymer grafting to GO/rGO surfaces (FT-IR, XPS, ToF-SIMS, quantitative solid-state ^{13}C NMR).

FT-IR, XPS, time-of-flight secondary ion mass spectrometry (ToF-SIMS) and solid-state ^{13}C NMR analysis were performed to in detail to further investigate the polymer grafting for both *grafting-to* and *grafting-from* approaches. For *grafting-to via* CuAAC, GO-PMMA (with PMMA M_n = 2,600 g/mol) and GO-PDEGA (with PMMA M_n = 2,700 g/mol) were investigated since they

showed the highest grafting ratios according to TGA. For *grafting-from*, PMMA and PDEGA grafted *via* SI-photoCMP/1-3 in a batch reactor were analyzed. All samples were compared to relevant blank GO/rGO-Initiator samples.

FT-IR provides qualitative information towards polymer grafting. GO sheets that were modified with PMMA and PDEGA chains show additional signals that can be directly assigned to the polymer stretching modes as shown in Figure S7. FT-IR confirms presence of the grafts on the GO sheets.

Further analysis was performed *via* ToF-SIMS which is very surface-sensitive technique with a probing depth of a few nm only. The mass spectra obtained by ToF-SIMS allow for a differentiation of several polymer layers based on characteristic molecular fragments. In this case, amongst several other, the $C_4H_5O_2^-$ fragment attributed to PMMA and the $C_2H_3O^-$ fragment attributed to PDEGA were detected. Figure 6 shows the intensity of the detected $C_4H_5O_2^-$ fragment for the different GO/rGO-derivatives. Since methyl methacrylates yield $C_4H_5O_2^-$ fragments among several other characteristic signals in SIMS, the highest intensity was observed for all GO-PMMA-based samples, proving the presence of PMMA on the surface. Differently, the side chain of grafted PDEGA yields strong $C_2H_3O^-$ signals, which is not applicable for grafted PMMA. After comparison the intensities of $C_2H_3O^-$ fragments (Figure 7), the highest was obtained for all GO-PDEGA-based samples, proving the presence of PDEGA on the surface.

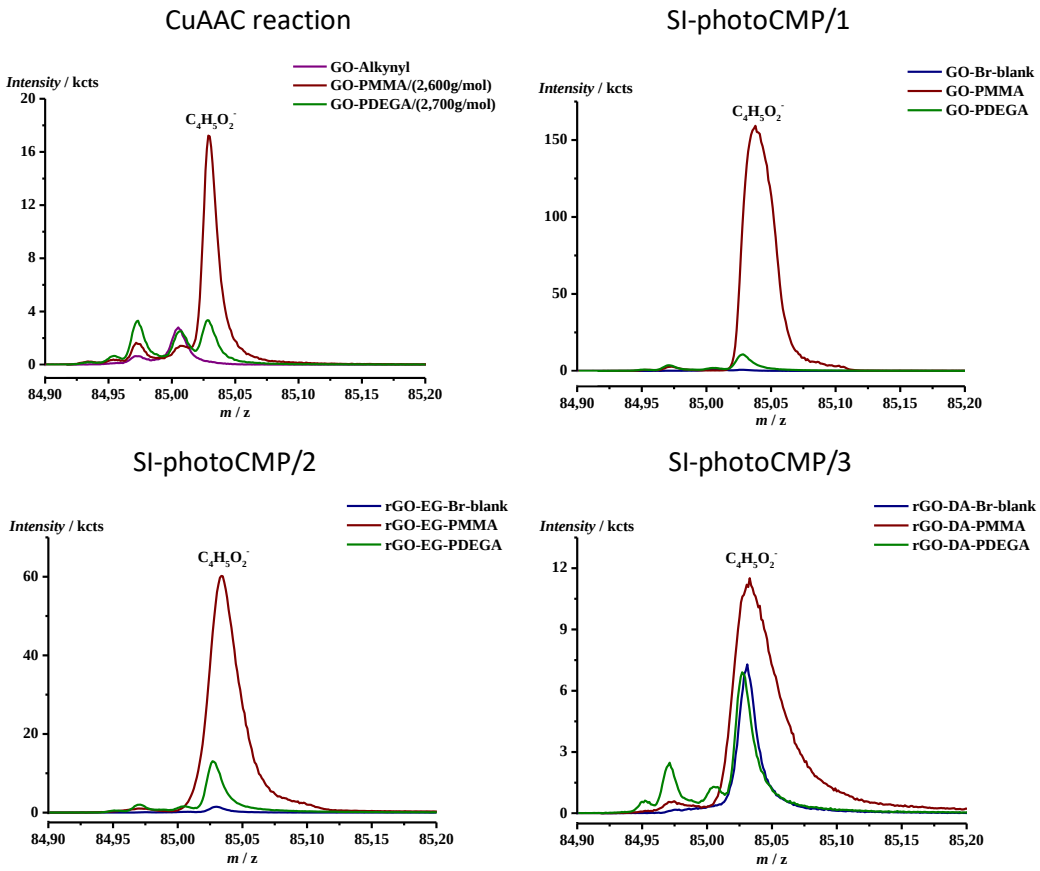

Figure 6. ToF-SIMS spectra of $C_4H_5O_2^-$ fragment of PMMA and PDEGA functionalized GO/rGO sheets *via* CuAAC reaction and SI-photoCMP procedures. Spectra compared to relevant blank samples.

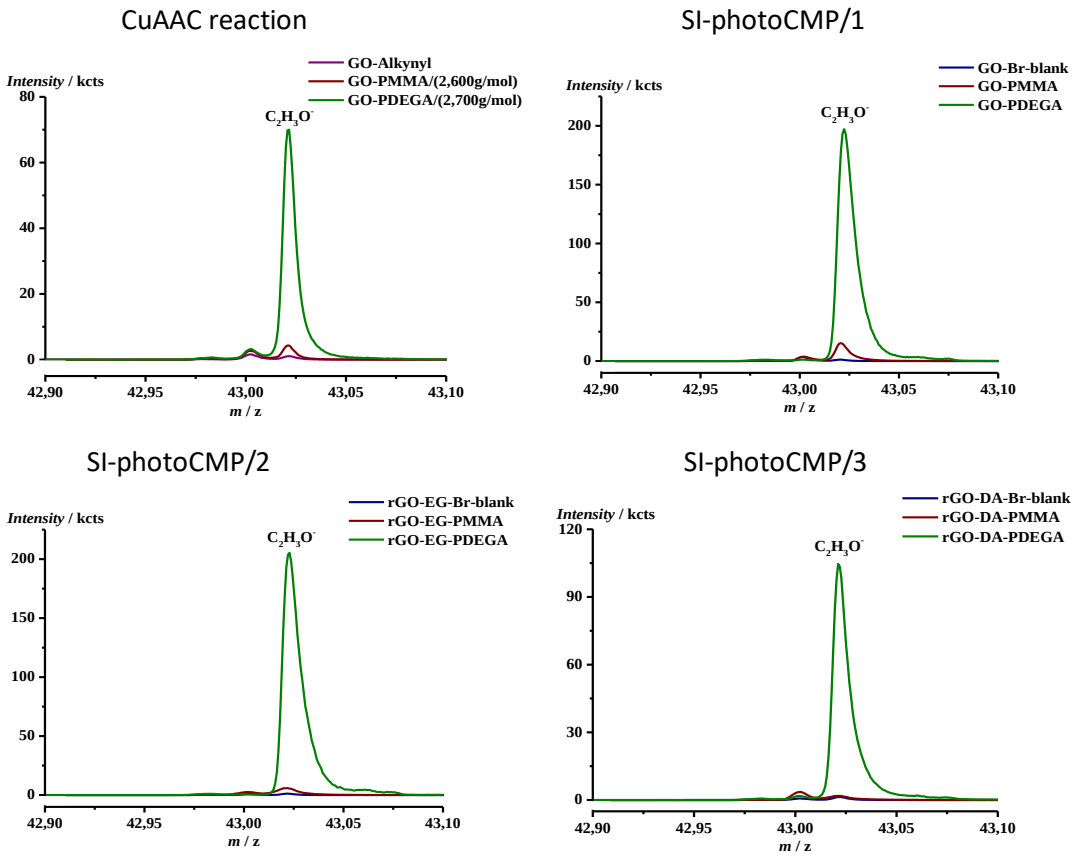

Figure 7. ToF-SIMS spectra of $C_2H_3O^-$ fragment of PMMA and PDEGA functionalized GO/rGO sheets *via* CuAAC reaction and SI-photoCMP procedures. Spectra are compared to relevant blank samples.

The high-resolution C 1s XPS spectra of the grafted polymers are depicted in Figure 8. The appearance of a C-Br signal at 70.1 eV (not shown, Br atomic % is represented instead in Table S1) confirms the successful introduction of an initiator molecule on the GO/rGO surface, as discussed above. After introducing the PMMA chains on the surface, the C 1s XPS spectra of the new materials can be deconvoluted into three components, C-C/C-H, C-O and O=C-O species at 285.0, 286.6, and 288.8 eV respectively, in accordance with the chemical composition of the grafted polymer. The close matching between the theoretical (3 : 1 : 1) and measured/fitted values in C 1s peak confirms the attachment of PMMA on the surface (Table S8). However, poor

matching of C-O peaks in GO-PMMA (M_n = 2,600 g/mol) sample was observed and can be explained by a low grafting density and therefore a signal stemming from both, PMMA and GO-Alkynyl. For PDEGA, the C 1s XPS spectra can be deconvoluted into three components, similar to PMMA but with given theoretical ratios 3 : 5 : 1, based on carbon chemical environment of PDEGA. Again, a close match between the theoretical and measured/fitted values was obtained for samples grafted with PDEGA (Table S8).

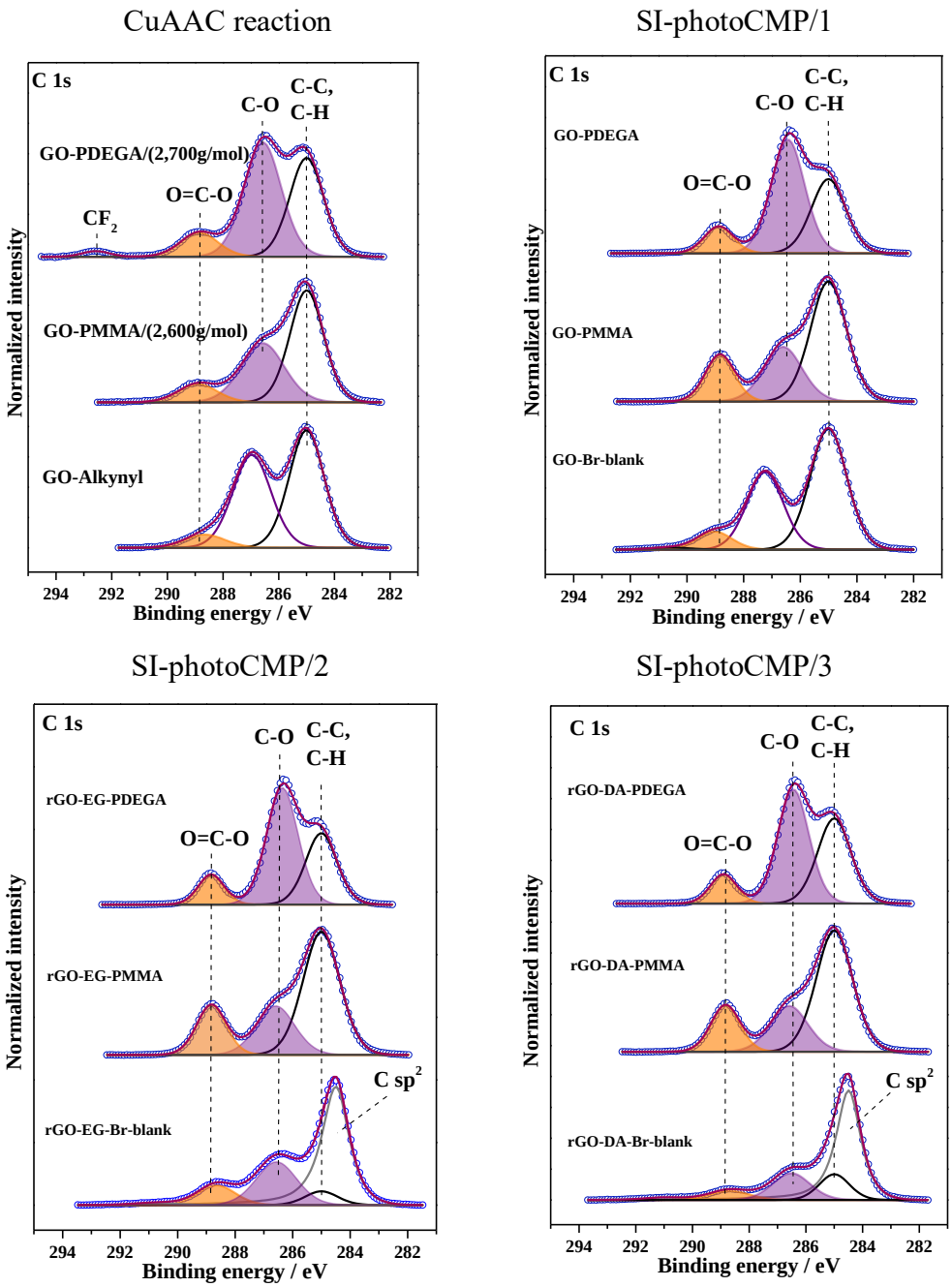

Figure 8. XPS spectra of PMMA and PDEGA functionalized GO/rGO sheets *via* CuAAC reaction and SI-photoCMP procedures. Spectra compared to relevant blank samples. The CF2 signal in the CuAAC reaction stems from sample contamination.

In a last step, solid-state ^{13}C NMR spectra were measured to analyze the structures of all GO/rGO-derivatives after grafting (Figure S8). In GO-PMMA, the appearance of additional resonance peaks are assigned to backbone CH_3 at 16 ppm, the quaternary C and CH_2 backbone at 45 ppm, O-CH_3 at 52 ppm and R-C(O)-OR at 178 ppm.[53] In GO-PDEGA, resonance signals of PDEGA chains are assigned to CH_3 at 15 ppm, CH and CH_2 backbone at 41 ppm, O-CH_2 at 69 ppm and R-C(O)-OR at 174 ppm. In the blank samples of ^{13}C NMR spectra, no high-intensity resonance signals from impurities were detected. It proves reliable TGA thermogram interpretation over mass loss and quantitative determination of polymer grafting on the GO/rGO surfaces.

Determination of the polymer grafting densities of GO/rGO surfaces from TGA.

To calculate the polymer grafting density on GO/rGO surfaces, first the graft chain length needs to be determined. While it is straightforward to characterize the average length and dispersity of the polymer chains in *grafting-to*, the same information is more cumbersome to obtain for *grafting-from* methods. To this end, grafted polymers were cleaved from the modified GO/rGO surfaces *via* base hydrolysis (to break the ester linkage) in order to analyze the molecular weight (distributions).[16] Due to the minimized steric effect,[4, 8a, 8b] longer polymer chains are expected compared to *grafting-to*. PMMA was cleaved from GO-PMMA, rGO-EG-PMMA and rGO-DA-PMMA, synthesized *via* SI-photoCMP/1-3 in a batch reactor. As a side reaction, ester groups present in the PMMA side chains (methyl group) are prone to hydrolyse under basic conditions, and therefore, were quenched *in situ* with methanol to restore the methyl ester side chains. Cleavage of PDEGA was not performed due to the longer and complexer side chains.

Figure S9 shows SEC analysis of the cleaved PMMA obtained from GO-PMMA, rGO-EG-PMMA and rGO-DA-PMMA UV-batch polymerizations (7.5 mmol catalyst concentration). The average

number molecular weights (M_n) observed were 35,200 g/mol, 40,300 g/mol and 29,200 g/mol respectively. Dispersities of the cleaved PMMA were observed in the range of $Đ$ = 1.40 (GO-PMMA) and $Đ$ =1.59 (rGO-EG-PMMA). The PMMA cleaved from rGO-EG-PMMA has higher dispersity and the high molecular weight shoulder, explained by an increase of viscosity, which causes a reduced stirring speed. Light does not penetrate deep through the mixture and polymerization occurs only at the irradiated parts. Therefore, a high stirring speed and efficient mixing is required. In addition, higher viscosity favors bimolecular radical termination events of growing polymer chains on the surface. PMMA has higher molecular weight brushes compared to PMMA, used in CuAAC. However, broader dispersities were observed by using SI-photoCMP to polymerize from the surface, compared to previously reported PMMA grafting *via* conventional thermally intiated SI-ATRP with M_n = 1,170 g/mol and $Đ$ = 1.09.[23]

The grafting density is defined as a number of attached polymer chains per unit surface area. The polymer grafting density on the surface was determined by TGA. Herein, the grafting density is shown as # carbons of graphene per grafted one polymer chain. By knowing the area of the benzene ring in graphene (0.0524 nm^2), the grafting density as a number of polymer chains per nm^2 of graphene can be calculated (Table 1).[54]

As discussed previously, in *grafting-to*, higher molecular weight polymers have slower diffusivity that results into lower grafting ratio.[46] Here, one PMMA chain (M_n = 2,600 g/mol) was grafted per 990 carbons of graphene and one PMMA chain (M_n = 7,100 g/mol) was grafted per 3,251 carbons of graphene (Table 1). A lower grafting efficiency was previously reported by using CuAAC conjugation where one PSt (M_n = 4,600 g/mol) chain was grafted to approximately 1,500 carbon atoms of graphene.[11] In another contribution, the CuAAC conjugation approach resulted in one PMMA chain (M_n = 2,415 g/mol) per 5,000 carbons of graphene.[54]

In general, higher grafting density is achieved using *grafting-from* approach, compared to *grafting-to*. Thus, one PMMA chain (M_n = 2,600 g/mol) was grafted per 990 carbons of graphene in CuAAC, while one PMMA chain (M_n = 40,300 g/mol) per 140 and one PMMA (M_n = 29,200 g/mol) per 248 carbons of graphene was grafted *via* SI-photoCMP/2 and SI-photoCMP/3, respectively. Those obtained grafting densities are much higher than previously reported SI-ATRP grafting results of one PSt chain (M_n = 60,000 g/mol) per 1,000 carbon atoms.[22] Differing from the general trend, less PMMA grafting was obtained using SI-photoCMP/1. Here, one PMMA chain was grafted per 990 and 2,010 carbons of graphene *via* CuAAC and SI-photoCMP/1, respectively (Table 1). This can be explained by the difference in grafted PMMA molecular weight of M_n = 2,600 g/mol (CuAAC) and M_n = 35,200 g/mol (SI-photoCMP/1) and low initiator concentration attached to the GO surface. It should be noted that the outcome of the grafting experiments also depends on the GO used in the respective experiments, since GO is a relatively heterogeneous material. To make data comparable, the above values are determined on the same batches of GO. Yet, tests with different batches of GO showed that the method is overall well reproducible and significant.

Table 1. Overview of grafting characteristics from the various methods used, determined from TGA.

Sample	**M_{nSEC}, (PMMA) g/mol**	**# carbons of graphene per grafted PMMA chain**	**# PMMA chains per nm^2 of graphene**
GO-PMMA/(2,600 g/mol)	2,600	990	0.12
GO-PMMA/(7,100 g/mol)	7,100	3,251	0.04

GO-PMMA (SI-photoCMP/1)	35,200	2,010	0.06
rGO-EG-PMMA (SI-photoCMP/2)	40,300	140	0.82
rGO-DA-PMMA (SI-photoCMP/3)	29,200	248	0.46

Sample	**M_{nSEC}, (PDEGA) g/mol**	**# carbons of graphene per grafted PDEGA chain**	**# PDEGA chains per nm^2 of graphene**
GO-PDEGA/(2,700 g/mol)	2,700	403	0.28
GO-PDEGA/(8,000 g/mol)	8,000	2,321	0.05

Dispersibility studies.

Properties such as the dispersibility of GO/rGO derivatives in a variety of solvents and matrixes can be optimized by tuning polymer type and molecular weight. The dispersibility of rGO compared to GO is poor in organic solvents. Thus, the influence on the dispersibility of rGO sheets was investigated after polymerization with hydrophobic PMMA and hydrophilic PDEGA chains *via* SI-photoCMP/3. RGO, rGO-DA-PMMA and rGO-DA-PDEGA were dispersed in deionized water, ethanol (EtOH), and chloroform ($CHCl_3$) *via* sonication (15 min, Figure 9). RGO-DA-PMMA is not dispersible in polar solvents (water) but has enhanced dispersibility in nonpolar solvents like chloroform (see Figure 9). Even 24 hours after sonication the PMMA modified sheets of rGO did not precipitate. In contrast, PDEGA is a more polar compared to PMMA. As a result, rGO-DA-PDEGA became better dispersible in ethanol as observed in Figure 9.

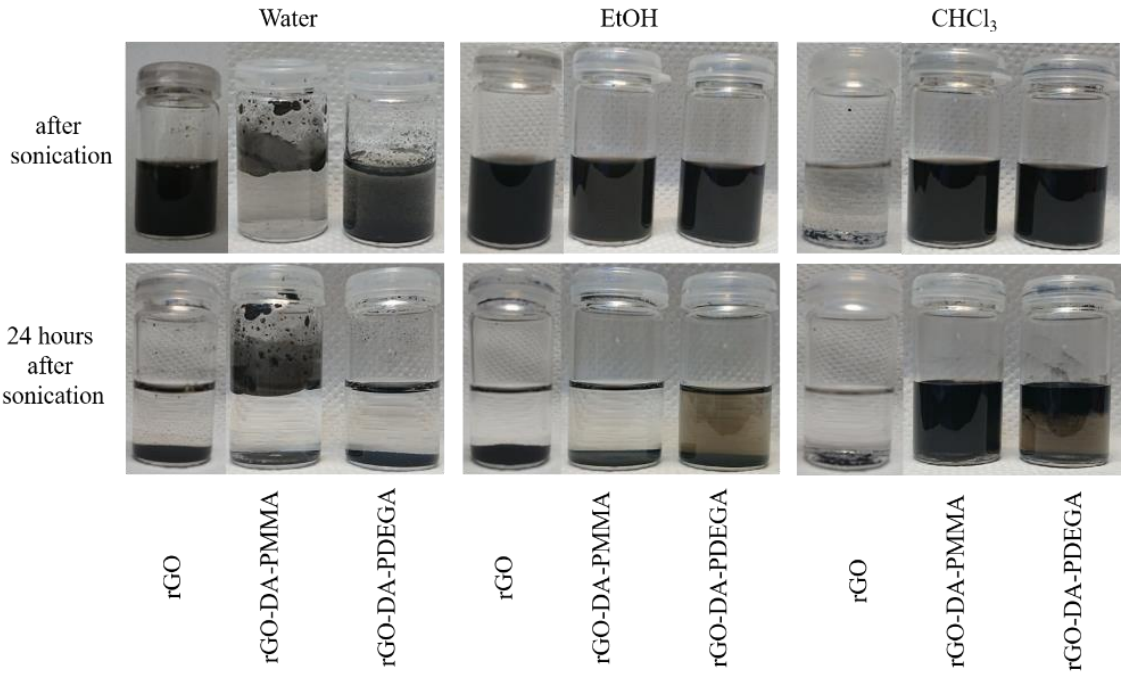

Figure 9. Dispersions of rGO, rGO-DA-PMMA and rGO-DA-PDEGA in various solvents with a concentration of 1 mg/mL.

Conclusions

The grafting of GO and rGO sheets with hydrophobic (PMMA) and hydrophilic (PDEGA) polymer chains *via* one *grafting-to* and three *grafting-from* approaches was investigated. SI-PhotoCMP proved a great tool for the synthesis of rGO-polymer materials under mild conditions (UV irradiation instead of elevated temperatures) with high polymer grafting density. The polymers were also grafted at reduced catalyst concentration (10 times for DEGA and 4 times for MMA grafting below standard protocol). In addition, the possibility to perform SI-photoCMP in both batch and continuous-flow reactors was demonstrated. Using a continuous-flow reactor allows to reduce the reaction time (from 24 hours to 1 hour) and upscale the system. Higher grafting densities were achieved by using *grafting-from* techniques (SI-photoCMP/2,3) due to the minimized steric factor compared to *grafting-to via* CuAAC. One PMMA chain (M_n = 2,600

g/mol) was grafted per 990 carbons of graphene *via* the *grafting-to* approach, calculated by TGA. In contrast, *via* SI-photoCMP, longer PMMA chains (M_n = 40,300 g/mol) and a higher grafting density (one PMMA chain per 140 carbons of graphene) were obtained. The PMMA grafted rGO has improved dispersibility in chloroform, compared to initial rGO, whilst grafted PDEGA to rGO has improved dispersibility in ethanol. The proposed SI-photoCMP technique comprises mild reaction conditions, short reaction time (1 hour in flow reactor) and high grafting densities with potential scalability. The pre-grafted polymer chains on the rGO surface improve its dispersibility in solvents and potentially in suitable polymer matrixes for production of evenly dispersed graphene sheets in polymer nanocomposites.

Acknowledgments

The authors kindly acknowledge Mariia Usichenko (Railian) (usichenko.mariia@gmail.com) for drawing the TOC image. The K-Alpha+ instrument was financially supported by the German Federal Ministry of Economics and Technology on the basis of a decision by the German Bundestag. The authors kindly acknowledge the CORNET project "GraphPOL: Graphene applications in polymers and polymer-based composites" for which funding was received from VLAIO with grant-number 140818.

Data Availability

The raw/processed data required to reproduce these findings cannot be shared at this time due to technical or time limitations.

References

[1] aJ. H. Koo, *Polymer nanocomposites*, McGraw-Hill Professional Pub., **2006**; bH. Fischer, *Materials Science and Engineering: C* **2003**, *23*, 763-772; cF. Hussain, M. Hojjati, M. Okamoto, R. E. Gorga, *Journal of composite materials* **2006**, *40*, 1511-1575.

[2] K. S. Novoselov, A. K. Geim, S. V. Morozov, D. Jiang, Y. Zhang, S. V. Dubonos, I. V. Grigorieva, A. A. Firsov, *science* **2004**, *306*, 666-669.

[3] H. Kim, A. A. Abdala, C. W. Macosko, *Macromolecules* **2010**, *43*, 6515-6530.

[4] H. J. Salavagione, G. Martínez, G. Ellis, *Macromolecular rapid communications* **2011**, *32*, 1771-1789.

[5] S. Park, R. S. Ruoff, *Nature nanotechnology* **2009**, *4*, 217.

[6] D. R. Dreyer, S. Park, C. W. Bielawski, R. S. Ruoff, *Chemical society reviews* **2010**, *39*, 228-240.

[7] aL. Rodriguez-Perez, M. Á. Herranz, N. Martin, *Chemical Communications* **2013**, *49*, 3721-3735; bA. Kasprzak, A. Zuchowska, M. Poplawska, *Beilstein journal of organic chemistry* **2018**, *14*.

[8] aA. Badri, M. R. Whittaker, P. B. Zetterlund, *Journal of Polymer Science Part A: Polymer Chemistry* **2012**, *50*, 2981-2992; bR. K. Layek, A. K. Nandi, *Polymer* **2013**, *54*, 5087-5103; cA. S. Nia, W. H. Binder, *Progress in Polymer Science* **2017**, *67*, 48-76.

[9] H. J. Salavagione, M. A. Gomez, G. Martinez, *Macromolecules* **2009**, *42*, 6331-6334.

[10] Z. Liu, J. T. Robinson, X. Sun, H. Dai, *Journal of the American Chemical Society* **2008**, *130*, 10876-10877.

[11] S. Sun, Y. Cao, J. Feng, P. Wu, *Journal of Materials Chemistry* **2010**, *20*, 5605-5607.

[12] H. He, C. Gao, *Chemistry of Materials* **2010**, *22*, 5054-5064.

[13] Z. Xu, C. Gao, *Macromolecules* **2010**, *43*, 6716-6723.

[14] L. Kan, Z. Xu, C. Gao, *Macromolecules* **2010**, *44*, 444-452.

[15] J. O. Zoppe, N. C. Ataman, P. Mocny, J. Wang, J. Moraes, H.-A. Klok, *Chemical reviews* **2017**, *117*, 1105-1318.

[16] D. Baskaran, J. W. Mays, M. S. Bratcher, *Angewandte Chemie* **2004**, *116*, 2190-2194.

[17] M. Fang, K. Wang, H. Lu, Y. Yang, S. Nutt, *Journal of Materials Chemistry* **2010**, *20*, 1982-1992.

[18] X. Xiong, L. Xue, J. Cui, *ACS Macro Letters* **2018**, *7*, 239-243.

[19] D. Goodman, J. N. Kizhakkedathu, D. E. Brooks, *Langmuir* **2004**, *20*, 6238-6245.

[20] aR. Feng, W. Zhou, G. Guan, C. Li, D. Zhang, Y. Xiao, L. Zheng, W. Zhu, *Journal of Materials Chemistry* **2012**, *22*, 3982-3989; bM. Kim, C. Lee, Y. D. Seo, S. Cho, J. Kim, G. Lee, Y. K. Kim, J. Jang, *Chemistry of Materials* **2015**, *27*, 6238-6248.

[21] M. H. Stenzel, C. Barner-Kowollik, *Materials Horizons* **2016**, *3*, 471-477.

[22] M. Fang, K. Wang, H. Lu, Y. Yang, S. Nutt, *Journal of Materials Chemistry* **2009**, *19*, 7098-7105.

[23] G. Goncalves, P. A. A. P. Marques, A. Barros-Timmons, I. Bdkin, M. K. Singh, N. Emami, J. Gracio, *Journal of Materials Chemistry* **2010**, *20*, 9927-9934.

[24] S. H. Lee, D. R. Dreyer, J. An, A. Velamakanni, R. D. Piner, S. Park, Y. Zhu, S. O. Kim, C. W. Bielawski, R. S. Ruoff, *Macromolecular Rapid Communications* **2010**, *31*, 281-288.

[25] aX. Pan, M. A. Tasdelen, J. Laun, T. Junkers, Y. Yagci, K. Matyjaszewski, *Progress in Polymer Science* **2016**, *62*, 73-125; bN. Corrigan, J. Yeow, P. Judzewitsch, J. Xu, C. A. J. M. Boyer, *Angewandte Chemie* **2018**.
[26] H. Kong, J. Song, J. Jang, *Environmental science & technology* **2010**, *44*, 5672-5676.
[27] P. Liu, J. Tian, W. Liu, Q. Xue, *Polymer international* **2004**, *53*, 127-130.
[28] J. Yan, B. Li, F. Zhou, W. Liu, *ACS Macro Letters* **2013**, *2*, 592-596.
[29] A. Bansal, A. Kumar, P. Kumar, S. Bojja, A. K. Chatterjee, S. S. Ray, S. L. Jain, *RSC Advances* **2015**, *5*, 21189-21196.
[30] aE. Baeten, J. J. Haven, T. Junkers, *Polymer Chemistry* **2017**, *8*, 3815-3824; bJ. Wegner, S. Ceylan, A. Kirschning, *Chemical Communications* **2011**, *47*, 4583-4592; cT. Junkers, B. Wenn, *Reaction Chemistry & Engineering* **2016**, *1*, 60-64.
[31] aK. Jähnisch, V. Hessel, H. Löwe, M. Baerns, *Angewandte Chemie International Edition* **2004**, *43*, 406-446; bA. Kirschning, W. Solodenko, K. Mennecke, *Chemistry–A European Journal* **2006**, *12*, 5972-5990; cB. P. Mason, K. E. Price, J. L. Steinbacher, A. R. Bogdan, D. T. McQuade, *Chemical reviews* **2007**, *107*, 2300-2318; dR. L. Hartman, K. F. Jensen, *Lab on a Chip* **2009**, *9*, 2495-2507; eC. Wiles, P. Watts, *European Journal of Organic Chemistry* **2008**, *2008*, 1655-1671; fK. Geyer, T. Gustafsson, P. H. Seeberger, *Synlett* **2009**, *2009*, 2382-2391; gD. Webb, T. F. Jamison, *Chemical Science* **2010**, *1*, 675-680.
[32] aJ. J. Haven, T. Junkers, *Chimica Oggi/Chemistry Today* **2018**, *36*, 42-44; bJ. J. Haven, T. Junkers, *European Journal of Organic Chemistry* **2017**, *2017*, 6474-6482; cM. Rubens, J. H. Vrijsen, J. Laun, T. Junkers, *Angewandte Chemie International Edition* **2019**, *58*, 3183-3187; dX. Hu, N. Zhu, Z. Fang, Z. Li, K. Guo, *European Polymer Journal* **2016**, *80*, 177-185.
[33] aA. Anastasaki, V. Nikolaou, Q. Zhang, J. Burns, S. R. Samanta, C. Waldron, A. J. Haddleton, R. McHale, D. Fox, V. Percec, P. Wilson, D. M. Haddleton, *Journal of the American Chemical Society* **2014**, *136*, 1141-1149; bM. Rolland, R. Whitfield, D. Messmer, K. Parkatzidis, N. P. Truong, A. Anastasaki, *ACS Macro Letters* **2019**, *8*, 1546-1551; cD. Konkolewicz, K. Schröder, J. Buback, S. Bernhard, K. Matyjaszewski, *ACS Macro Letters* **2012**, *1*, 1219-1223; dR. Whitfield, K. Parkatzidis, M. Rolland, N. P. Truong, A. Anastasaki, *Angewandte Chemie International Edition* **2019**, *58*, 13323-13328.
[34] N. Zhu, X. Hu, Z. Fang, K. Guo, *ChemPhotoChem* **2018**, *2*, 831-838.
[35] G. Ramakers, A. Krivcov, V. Trouillet, A. Welle, H. Möbius, T. Junkers, *Macromolecular Rapid Communications* **2017**, *38*, 1700423.
[36] aE. Rossi, T. Carofiglio, A. Venturi, A. Ndobe, M. Muccini, M. Maggini, *Energy & Environmental Science* **2011**, *4*, 725-727; bH. Seyler, W. W. Wong, D. J. Jones, A. B. Holmes, *The Journal of organic chemistry* **2011**, *76*, 3551-3556; cS. Silvestrini, D. Dalle Nogare, T. Carofiglio, E. Menna, P. Canu, M. Maggini, *European Journal of Organic Chemistry* **2011**, *2011*, 5571-5576.
[37] aP. Salice, D. Fenaroli, C. C. De Filippo, E. Menna, G. Gasparini, M. Maggini, *chimica oggi/Chemistry Today* **2012**, *30*; bP. Salice, E. Rossi, A. Pace, P. Maity, T. Carofiglio, E. Menna, M. Maggini, *Journal of Flow Chemistry* **2014**, *4*, 79-85; cJ. H. Bartha-Vári, M. I. Toşa, F. D. Irimie, D. Weiser, Z. Boros, B. G. Vértessy, C. Paizs, L. Poppe, *ChemCatChem* **2015**, *7*, 1122-1128; dS. Melendi, S. Bonyadi, P. Castell, M. Martinez, M. Mackley, *Chemical engineering science* **2012**, *84*, 544-551; eP. Salice, P. Maity, E.

Rossi, T. Carofiglio, E. Menna, M. Maggini, *Chemical Communications* **2011**, *47*, 9092-9094.
[38] S. Silvestrini, C. C. De Filippo, N. Vicentini, E. Menna, R. Mazzaro, V. Morandi, L. Ravotto, P. Ceroni, M. Maggini, *Chemistry of Materials* **2018**, *30*, 2905-2914.
[39] Y. Pan, H. Bao, N. G. Sahoo, T. Wu, L. Li, *Advanced Functional Materials* **2011**, *21*, 2754-2763.
[40] Z. Jin, T. P. McNicholas, C.-J. Shih, Q. H. Wang, G. L. Paulus, A. J. Hilmer, S. Shimizu, M. S. Strano, *Chemistry of Materials* **2011**, *23*, 3362-3370.
[41] aY.-M. Chuang, B. Wenn, S. Gielen, A. Ethirajan, T. Junkers, *Polymer Chemistry* **2015**, *6*, 6488-6497; bS. Railian, B. Wenn, T. Junkers, *Journal of Flow Chemistry* **2016**, *6*, 260-267.
[42] aA. Coats, J. Redfern, *Analyst* **1963**, *88*, 906-924; bK. Chrissafis, D. Bikiaris, *Thermochimica Acta* **2011**, *523*, 1-24.
[43] D. N. Benoit, H. Zhu, M. H. Lilierose, R. A. Verm, N. Ali, A. N. Morrison, J. D. Fortner, C. Avendano, V. L. Colvin, *Analytical chemistry* **2012**, *84*, 9238-9245.
[44] T. Wu, K. Efimenko, J. Genzer, *Journal of the american chemical society* **2002**, *124*, 9394-9395.
[45] L. C. Moh, M. D. Losego, P. V. Braun, *Langmuir* **2011**, *27*, 3698-3702.
[46] M. Kim, S. Schmitt, J. Choi, J. Krutty, P. Gopalan, *Polymers* **2015**, *7*, 1346-1378.
[47] M. Peeters, S. Kobben, K. Jiménez-Monroy, L. Modesto, M. Kraus, T. Vandenryt, A. Gaulke, B. van Grinsven, S. Ingebrandt, T. Junkers, *Sensors and Actuators B: Chemical* **2014**, *203*, 527-535.
[48] J. L. Bahr, J. M. Tour, *Chemistry of Materials* **2001**, *13*, 3823-3824.
[49] E. Rommozzi, M. Zannotti, R. Giovannetti, C. D'Amato, S. Ferraro, M. Minicucci, R. Gunnella, A. Di Cicco, *Catalysts* **2018**, *8*, 598.
[50] J. Laun, M. Vorobii, A. de los Santos Pereira, O. Pop-Georgievski, V. Trouillet, A. Welle, C. Barner-Kowollik, C. Rodriguez-Emmenegger, T. Junkers, *Macromolecular rapid communications* **2015**, *36*, 1681-1686.
[51] B. Wenn, M. Conradi, A. D. Carreiras, D. M. Haddleton, T. Junkers, *Polymer Chemistry* **2014**, *5*, 3053-3060.
[52] aK. Qi, Y. Sun, H. Duan, X. Guo, *Corrosion Science* **2015**, *98*, 500-506; bL. Ren, S. Huang, C. Zhang, R. Wang, W. W. Tjiu, T. Liu, *Journal of Nanoparticle Research* **2012**, *14*, 940.
[53] T. E. Motaung, A. S. Luyt, F. Bondioli, M. Messori, M. L. Saladino, A. Spinella, G. Nasillo, E. Caponetti, *Polymer Degradation and Stability* **2012**, *97*, 1325-1333.
[54] Y.-S. Ye, Y.-N. Chen, J.-S. Wang, J. Rick, Y.-J. Huang, F.-C. Chang, B.-J. Hwang, *Chemistry of Materials* **2012**, *24*, 2987-2997.

TOC figure

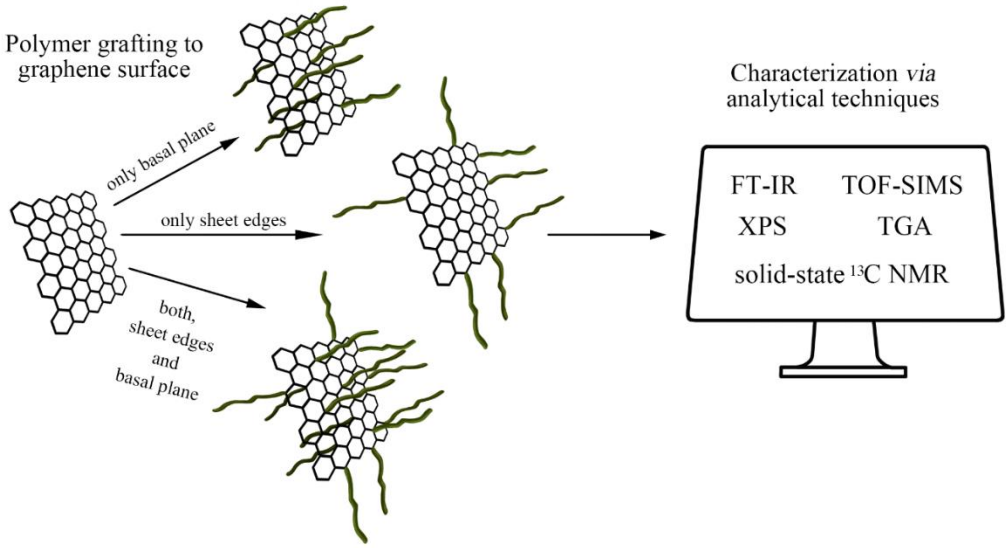
Polymer grafting to graphene surface
only basal plane
only sheet edges
both, sheet edges and basal plane
Characterization *via* analytical techniques
FT-IR
TOF-SIMS
XPS
TGA
solid-state ^{13}C NMR

Supporting Information

Photo-Induced Copper-Mediated (Meth)Acrylate Polymerization towards Graphene Oxide and Reduced Graphene Oxide Modification

Svitlana Railian,[1] Joris J. Haven,[2] Lowie Maes,[1] Dries De Sloovere,[3,4,5] Vanessa Trouillet,[6,7] Alexander Welle,[7,8] Peter Adriaensens,[5,9] Marlies K. Van Bael,[3,4,5] An Hardy,[3,4,5] Wim Deferme,[5,10] and Tanja Junkers[1,2*]

[1] Polymer Reaction Design group, UHasselt – Institute for Materials Research, Agoralaan, 3590 Diepenbeek, Belgium.

[2] School of Chemistry, Monash University, 19 Rainforest Walk, Clayton VIC 3800, Australia

[3] UHasselt – Institute for Materials Research, Inorganic and Physical Chemistry, Agoralaan, 3590 Diepenbeek, Belgium.

[4] Energyville, Thor Park 8320, B-3600 Genk, Belgium

[5] IMEC vzw – Division IMOMEC, Wetenschapspark 1, 3590 Diepenbeek, Belgium

[6] Institute for Applied Materials (IAM), Karlsruhe Institute of Technology (KIT), Hermann-von-Helmholtz-Platz 1, 76344 Eggenstein-Leopoldshafen, Germany

[7] Karlsruhe Nano Micro Facility (KNMF), Karlsruhe Institute of Technology (KIT), Hermann-von-Helmholtz-Platz 1, 76344 Eggenstein-Leopoldshafen, Germany

[8] Institute of Functional Interfaces, Karlsruhe Institute of Technology (KIT), Hermann-von-Helmholtz-Platz 1, 76344 Eggenstein-Leopoldshafen, Germany

[9] UHasselt – Institute for Materials Research, Nuclear Magnetic Resonance Spectroscopy Group, Agoralaan 1, building D, 3590 Diepenbeek, Belgium.

[10] UHasselt – Institute for Materials Research, Wetenschapspark 1, 3590 Diepenbeek, Belgium.

* Corresponding Author: Tanja Junkers, Email: tanja.junkers@uhasselt.be, Homepage: www.polymatter.net, Twitter: @prd_group

Experimental

Materials:

All chemicals were of reagent grade or higher and were used as received unless otherwise specified. Graphene/graphite nanoplatelets (Avanzare), reduced graphene oxide (rGO, Avanzare), triethylamine (TEA, Acros, 99%), 2-bromoisobutyryl bromide (Alfa Aesar, 97%), propargyl amine (J&K Scientific, 98%), N,N′-dicyclohexylcarbodiimide (DCC, Acros, 99%), 4-dimethylaminopyridine (DMAP, Acros, 99%), thionyl chloride ($SOCl_2$, Acros, 99.7%), ethylene glycol (EG, Fisher, 99+%), 2-(4-aminophenyl)ethanol (Fisher Scientific, 97%), isoamyl nitrite (Alfa Aesar, 97%, stab. with 0.2% anhyd. sodium carbonate), sodium azide (NaN_3, Acros, 99%, extra pure), ethyl 2-bromoisbutyrate (EBiB, Alfa Aesar, 98+%), N,N,N′,N″,N″-Pentamethyl-di-ethylenetriamine (PMDETA, Aldrich, 99%), copper (II) bromide ($CuBr_2$, Sigma-Aldrich, 99%), sulfuric acid (H_2SO_4, Fisher, >95%), phosphoric acid (H_3PO_4, Acros, 85%), hydrochloric acid (HCl, Fisher, ~37%), potassium permanganate ($KMnO_4$, Acros, 99%), hydrogen peroxide (H_2O_2, Acros, 35%), ethanol (EtOH, Fisher, absolute), methanol (MeOH, Fisher, analytical reagent grade), N,N-Dimethylformamide (DMF, Fisher, analytical reagent grade), tetrahydrofuran (THF, Fisher, laboratory reagent grade), chloroform ($CHCl_3$, Fisher, laboratory reagent grade), dichloromethane (CH_2Cl_2, Fisher, laboratory reagent grade), ethanol (EtOH, VWR, absolute, denatured with 3% isopropanol), methanol (MeOH, VWR, technical grade), diethyl ether (VWR, technical grade) were used as received.

Tris-(2-(dimethylamino)ethyl)amine (Me_6TREN)[1] and 2-hydroxyethyl 2′-methyl-2′-bromopropionate (HMB)[2] were synthesized following literature procedures. Copper (I) bromide (CuBr, Sigma-Aldrich, 98%) was washed with acetic acid at 80 °C for 18 h to remove any soluble

oxidized species before being filtered, washed with absolute ethanol, brought to pH 7, washed with ethyl ether, and then dried under vacuum.

Methyl methacrylate (MMA, Acros, 99%) and di(ethylene glycol) ethyl ether acrylate (DEGA, TCI, 98%) were deinhibited over a column of activated basic alumina prior to use.

Methods:

^{1}H NMR (nuclear magnetic resonance) spectra were recorded in deuterated chloroform by applying a pulse delay of 12 s and 64 scans with Oxford Instruments Ltd. NMR spectrometers (300 and 400 MHz).

High-resolution solid-state NMR. Solid-state ^{13}C NMR spectra were acquired on an Agilent VNMRS DirectDrive 400 MHz spectrometer (9.4 T wide bore magnet) equipped with a T3HX 3.2 mm probe. Magic angle spinning (MAS) was performed at 16 kHz and the aromatic signal of hexamethylbenzene was used to calibrate the carbon chemical shift scale (132.1 ppm). Acquisition parameters were used: a spectral width of 50 kHz, a 90° pulse length of 2.5 µs, an acquisition time of 15 ms, a recycle delay time of 90 s and 2500 accumulations. High power proton dipolar decoupling during the acquisition time was set to 80 kHz.

XPS (X-ray photoelectron spectroscopy) measurements were performed using a K-Alpha+ XPS spectrometer (ThermoFisher Scientific, East Grinstead, UK). Data acquisition and processing using the Thermo Avantage software is described elsewhere.[3] All samples were analyzed using a microfocused, monochromated Al Kα X-ray source (400 µm spot size). The K-Alpha+ charge compensation system was employed during analysis, using electrons of 8 eV energy, and low-energy argon ions to prevent any localized charge build-up. The spectra were fitted with one or more Voigt profiles (binding energy uncertainty: ±0.2 eV) and Scofield sensitivity factors[4] were

applied for quantification. All spectra were referenced to the C 1s peak attributed to C–C, C–H at 285.0 eV binding energy which has been controlled by means of the well-known photoelectron peaks of metallic Cu, Ag, and Au, respectively.

ToF-SIMS (time-of-flight secondary ion mass spectrometry) was performed on a TOF.SIMS5 instrument (IONTOF GmbH, Münster, Germany). This spectrometer is equipped with a Bi cluster primary ion source and a reflectron type time-of-flight analyzer. UHV base pressure was $< 5 \cdot 10^{-9}$ mbar. For high mass resolution, the Bi source was operated in the "high current bunched" mode providing short Bi_3^+ primary ion pulses at 25 keV energy, a lateral resolution of approx. 4 µm, a target current of 0.25 pA. The short pulse length of 1.1 ns allowed for high mass resolution. The primary ion beam was rastered across a 500 × 500 μm^2 field of view on the sample, and 128 × 128 data points were recorded. Primary ion doses were kept below 10^{11} ions·cm^{-2} (static SIMS limit). If charge compensation was necessary an electron flood gun providing electrons of 21 eV was applied and the secondary ion reflectron tuned accordingly. Spectra were calibrated on the omnipresent C^-, C_2^-, C_3^-, or on the C^+, CH^+, CH_2^+, and CH_3^+ peaks. Based on these datasets the chemical assignments for characteristic fragments were determined.

Analytical SEC (size exclusion chromatography) was performed on a Tosoh EcoSEC HLC-8320GPC, comprising an autosampler, a PSS guard column SDV (50 × 7.5 mm), followed by three PSS SDV analytical linear XL (5 µm, 300 × 7.5 mm) columns thermostatted at 40 °C (column molecular weight range: 1×10^2 to 1×10^6 g/mol), and a differential refractive index detector (Tosoh EcoSEC RI) using THF as the eluent with a flow rate of 1 mL/min. Toluene was used as a flow marker. Calibration was performed using linear narrow polystyrene (PSt) standards from PSS Laboratories in the range of 470 g/mol to 7.5×10^6 g/mol. For the analysis, the following MHKS

parameters were used: for MMA, $\alpha = 0.731$, $K = 7.56 \times 10^{-5}$ dL/g in THF at 30 °C [5] and for DEGA, $\alpha = 0.714$, $K = 13.63 \times 10^{-5}$ dL/g, THF 30 °C at 633 nm for PSt.[6]

ATR FT-IR (attenuated total reflection fourier-transform infrared spectroscopy) spectra were collected on a Brucker Tensor 27 FT-IR spectrophotometer (32 scans and nominal resolution 4 cm^{-1}).

TGA (thermo gravimetric analysis) was performed on TA instruments Q500, heating 3-4 mg of the sample at a heating rate of 10 °C·min^{-1} under nitrogen atmosphere (flow of 90 mL min^{-1}).

Continuous photoflow reactors were built up out of a 4.5-m perfluoroalkoxy (PFA) tubing (Advanced Polymer Tubing GmbH; outer diameter, 1/16″; inner diameter, 0.75 mm; reactor volume, 2 mL) wrapped around a Vilber Lourmat 15 W UV light tube ($\lambda_{max} \sim 365$ nm). A syringe pump (Chemyx Fusion 100) was used to inject the reaction solutions into the reactor. The lamp heated the reactions to a temperature between 50 and 55 °C. All connections used were purchased from Upchurch Scientific and were made out of polyether ether ketone (PEEK).

The batch reactor was used as a UV nail gel curing lamp ($\lambda_{max} \sim 365$ nm) equipped with four 9W bulbs.

SEM (scanning electron microscopy) was measured using FEI Quanta 200F Field Emission Gun Scanning Electron Microscope (FEG-SEM, Thermo Fisher Scientific, Waltham, MA, USA) in back-scattered electron (BSE) mode for an optimized z-contrast. The samples were observed at magnifications of 2000 x.

Synthesis procedures:

The general synthesis procedure of GO. GO was prepared from graphene/graphite nanoplatelets according to the improved Hummer's method.[7] A mixture of the acids H_2SO_4/H_3PO_4 (9/1 = 360/40 mL) was added to a mixture of graphene/graphite flakes (3.0 g, 1 eq.) and $KMnO_4$ (18.0 g,

6 eq.) and kept stirring the mixture for 12 h at 50 °C. The reaction was cooled down and poured onto ice (400 mL) with 30% H_2O_2 (3 mL). The mixture was centrifuged (4000 rpm for 15 min), and the supernatant was decanted away. The remaining solid material was washed with repeated cycles of centrifugation and rinsing with 30% HCl, 5% HCl, distilled water, ethanol, and diethyl ether. The final product was dried under vacuum at 40 °C.

"Grafting-to" procedure - CuAAC approach

Synthesis of GO-Alkynyl. GO-Alkynyl was prepared according to the synthesis procedure previously reported.[8] GO (0.5 g) was dispersed in DMF (250 mL) by 1 hour sonication in a bath sonicator. Then propargyl amine (1.36 g, 1 eq.) was added and dissolved by stirring. DCC (dicyclohexylcarbodiimide) (20 g, 10 eq.) and DMAP (4-dimethylaminopyridine) (1.5 g, 1 eq.) were gradually added to the flask during 20 min and the mixture was kept stirred for 16 h at room temperature. For workup, most of DMF was evaporated under reduced pressure. The remaining solid material was filtered through a polytetrafluoroethylene (PTFE) membrane with a pore size 0.45 µm and washed with an excess of dichloromethane and chloroform. The final product was dried under vacuum at 40 °C.

Synthesis of PMMA-N_3. PMMA-Br was prepared according to the synthesis procedure previously reported.[9] EBiB (Ethyl 2-bromoisbutyrate) (0.732 g, 1 eq.), $CuBr_2$ (0.034 g, 0.04 eq.), PMDETA (0.085 g, 0.13 eq.), MMA (10 mL, 25 eq.) and DMF/MeOH solvent mixture (4/1 = 8/2 mL) were mixed in a 20 mL vial, corked with rubber stopper, sealed with parafilm and degassed by purging with nitrogen for 15 min. Subsequently, the vial was placed in a UV nail lamp with a stirrer plate for 6 hours. After the polymerization, the mixture was diluted with DMF and passed through a basic alumina column to remove the copper catalyst. The excess of DMF was evaporated

under reduced pressure and PMMA-Br was dried under vacuum at 40 °C. The conversion was calculated *via* ^{1}H NMR and molecular weight was obtained *via* SEC. The conversion was reached 48.5% and M_n = 2,600 g/mol with dispersity Đ = 1.33. The obtained PMMA-Br (2.5 g, 1 eq.) and NaN_3 (0.13 g, 2 eq.) were dissolved in DMF (15 mL) and allowed to react 24 hours at 24 °C. The mixture was diluted with DMF and passed through a basic alumina column to remove the unreacted NaN_3 and sodium salt. The excess of DMF was evaporated under reduced pressure and PMMA-N_3 was dried under vacuum at 40 °C. M_n = 2,600 g/mol and dispersity Đ = 1.34. The similar reaction conditions were used to obtain longer polymer chain with targeted DP = 100. The conversion was 47% and M_n (PMMA-Br) = 7,100 g/mol with dispersity Đ = 1.23 and M_n (PMMA-N_3) = 7,100 g/mol with dispersity Đ = 1.23.

Synthesis of PDEGA-N_3. PDEGA-Br was prepared according to the synthesis procedure previously reported.[10] HMB (2-hydroxyethyl 2′-methyl-2′bromopropionate) (0.702 g, 1 eq.), $CuBr_2$ (0.016 g, 0.02 eq.), Me_6TREN (0.099 g, 0.12 eq.), DEGA (10 mL, 15 eq.) and H_2O/EtOH solvent mixture (1/1 = 5/5 mL) were mixed in a 20-mL vial, corked with rubber stopper, sealed with parafilm and degassed by purging with nitrogen for 15 min. Subsequently, the vial was placed in a UV nail lamp with a stirrer plate for 3 hours. After the polymerization, the mixture was diluted with EtOH and passed through a basic alumina column to remove the copper catalyst. The excess of EtOH was evaporated under reduced pressure and PDEGA-Br was dried under vacuum at 40 °C. The conversion was calculated *via* ^{1}H NMR and molecular weight was obtained *via* SEC. The conversion reached 98% and M_n = 2,600 g/mol with dispersity Đ = 1.23. The obtained PDEGA-Br (2.5 g, 1 eq.) and NaN_3 (0.125 g, 2 eq.) were dissolved in DMF (15 mL) and allowed to react 24 hours at 24 °C. The mixture was diluted with DMF and passed through a basic alumina column to remove the unreacted NaN_3 and sodium salt. The excess of DMF was evaporated under reduced

pressure and PDEGA-N_3 was dried under vacuum at 40 °C. M_n = 2,700 g/mol and dispersity Đ = 1.23. The similar reaction conditions were used to obtain longer polymer chains with targeted DP = 50. The conversion was 97% and M_n (PDEGA-Br) = 7,800 g/mol with dispersity Đ = 1.36, while M_n (PDEGA- N_3) = 8,000 g/mol with dispersity Đ = 1.34.

Synthesis of GO-PMMA. GO-Alkynyl (0.1 g), PMMA-N_3 (2.0 g, 1 eq.) and PMDETA (*N,N,N',N'',N*''-pentamethyl-di-ethylenetriamine) (0.638 g, 5 eq.) were loaded into a 50 mL Schlenk flask, dissolved in DMF (30 mL) and degassed four times by freeze-vacuum-thaw cycles. CuBr (0.528 g, 5 eq.), was added in the presence of argon atmosphere. The mixture was stirred for 48 h at room temperature. The obtained product was filtered through a RC membrane with pore size 0.45 μm and washed with an excess of THF, EtOH and distilled water and then dried under vacuum at 40 °C.

Synthesis of GO-PDEGA. GO-Alkynyl (0.1 g), PDEGA-N_3 (2.0 g, 1 eq.) and PMDETA (N,N,N',N'',N''-pentamethyl-di-ethylenetriamine) (0.637 g, 5 eq.) were charged into a 50 mL Schlenk flask, dissolved in DMF (30 mL) and degassed four times by freeze-vacuum-thaw cycles. CuBr (0.527 g, 5 eq.), was added in the presence of argon atmosphere. The rest of the synthesis procedure follows as GO-PMMA.

"Grafting-from" procedure - SI-photoCMP/1 approach

Synthesis of GO-Br. GO-Br was prepared according to the synthesis procedure previously reported.[11] GO (0.5 g) and THF (100 mL) were loaded in three-neck round bottom flask and sonicated 1 hour in a bath sonicator. The mixture was treated with TEA (triethylamine) (10 mL), placed in an ice bath and degassed *via* purging with argon. 2-bromoisobutyryl bromide (2.5 mL) was added dropwise *via* dropping funnel and stirred overnight. The obtained product was filtered

through a RC membrane with pore size 0.45 μm and washed with an excess of chloroform, THF, and distilled water and then dried under vacuum at 40 °C.

Synthesis of GO-PMMA in batch reactor. GO-Br (0.1 g), $CuBr_2$ (0.034 g, 0.04 eq.) and DMF/MeOH solvent mixture (4/1 = 8/2 mL) were mixed in a 20-mL vial and sonicated 1 hour in sonication bath. Subsequently, PMDETA (0.085 g, 0.13 eq.) and MMA (10 mL, 25 eq.) were added. The vial with the reaction mixture was corked with a rubber stopper, sealed with parafilm and degassed by purging with nitrogen for 30 min and placed in a UV nail lamp with a stirrer plate and let it react for 24 hours. After the polymerization, the mixture was diluted with THF, filtered through the RC membrane with pore size 0.45 μm and washed with an excess of THF, EtOH and distilled water and then dried under vacuum at 40 °C.

Synthesis of GO-PMMA in batch reactor at lower catalyst concentration. GO-Br (0.1 g), $CuBr_2$ (0.008 g, 0.01 eq.) and DMF/MeOH solvent mixture (4/1 = 8/2 mL) were mixed in a 20-mL vial and sonicated 1 hour in sonication bath. Subsequently, PMDETA (0.021 g, 0.032 eq.) and MMA (10 mL, 25 eq.) were added. The rest of the synthesis procedure follows as synthesis of GO-PMMA in batch reactor.

Synthesis of GO-PMMA in flow reactor. GO-Br (0.1 g), $CuBr_2$ (0.034 g, 0.04 eq.) and DMF/MeOH solvent mixture (4/1 = 8/2 mL) were mixed in a 20-mL vial and sonicated 1 hour in sonication bath. Subsequently, PMDETA (0.085 g, 0.13 eq.) and MMA (10 mL, 25 eq.) were added. Flask with reaction mixture was degassed by purging with nitrogen for 30 min. Inside the 20 ml Normject plastic syringe, six PTFE-coated octagonal stir bars 5 mm long with 2 mm in diameter were loaded. The syringe was flushed 5 times with nitrogen gas and the reaction mixture was loaded and placed in the syringe pump. The syringe pump was used to deliver the reaction mixture. Above the syringe pump, the stirring plate was placed in order to prevent GO-Initiator

from precipitation. The residence time of 1 hour was used by choosing the flow rate of 0.033 mL/min. After reaction of polymerization, the mixture was diluted with THF, filtered through a RC membrane with pore size 0.45 μm and washed with an excess of THF, EtOH and distilled water and then dried under vacuum at 40 °C.

Synthesis of GO-PDEGA in batch reactor. GO-Br (0.1 g), $CuBr_2$ (0.024 g, 0.02 eq.) and H_2O/EtOH solvent mixture (1/1 = 5/5 mL) were mixed in a 20-mL vial and sonicated 1 hour in the sonication bath. Subsequently, Me_6TREN (0.150 g, 0.12 eq.) and DEGA (10 mL, 10 eq.) were added. The rest of the synthesis procedure follows as synthesis of GO-PMMA in batch reactor.

Synthesis of GO-PDEGA in batch reactor at lower catalyst concentration. GO-Br (0.1 g), $CuBr_2$ (0.002 g, 0.002 eq.) and H_2O/EtOH solvent mixture (1/1 = 5/5 mL) were mixed in a 20-mL vial and sonicated 1 hour in the sonication bath. Subsequently, Me_6TREN (0.015 g, 0.012 eq.) and DEGA (10 mL, 10 eq.) were added. The rest of the synthesis procedure follows as synthesis of GO-PMMA in batch reactor.

Synthesis of GO-PDEGA in flow reactor. GO-Br (0.1 g), $CuBr_2$ (0.024 g, 0.02 eq.) and H_2O/EtOH solvent mixture (1/1 = 5/5 mL) were mixed in a 20-mL brown volumetric flask and sonicated 1 hour in the sonication bath. Subsequently, Me_6TREN (0.150 g, 0.12 eq.) and DEGA (10 mL, 10 eq.) were added. The rest of the synthesis procedure follows as synthesis of GO-PMMA in flow reactor.

Synthesis of GO-Br-blank. GO-Br (0.1 g), $CuBr_2$ (0.024 g, 0.02 eq.) and H_2O/EtOH solvent mixture (1/1 = 5/5 mL) were mixed in a 20-mL vial and sonicated 1 hour in the sonication bath. The rest of the synthesis procedure follows as synthesis of GO-PMMA in batch reactor.

"Grafting-from" procedure - SI-photoCMP/2 approach

Synthesis of rGO-EG-OH. rGO-EG-OH was prepared according to the synthesis procedure.[12] GO (0.5 g) was suspended in $SOCl_2$ (50 mL) and stirred for 24 h at 65 °C in a round-bottom flask equipped with a condenser, N_2 inlet and stirring bar. Upon this, excess $SOCl_2$ was removed by centrifugation and the remaining solid material was washed with repeated cycles of centrifugation and rinsing with rinsing using THF. The resulting solid was suspended in ethylene glycol (50 mL) in a round-bottom flask equipped with a condenser and stirred for 48 h at 120 °C. For workup, unreacted ethylene glycol was removed by centrifugation and the remaining solid material was washed with repeated cycles of centrifugation and rinsing with rinsing using THF and then dried under vacuum at 40 °C.

Synthesis of rGO-EG-Br, rGO-EG-Br-blank, rGO-EG-PMMA and rGO-EG-PDEGA in batch reactor, rGO-EG-PMMA and rGO-EG-PDEGA in batch reactor at lower catalyst concentration and rGO-EG-PMMA and rGO-EG-PDEGA in flow reactor are the same as SI-photoCMP/1 approach.

"Grafting-from" procedure - SI-photoCMP/3 approach

Synthesis of rGO-DA-OH. rGO-DA-OH was prepared according to the synthesis procedure.[13] rGO (0.5 g) was suspended in deionized water (125 mL) in a round-bottom flask and sonicated 1 hour in the sonication bath. The mixture was transferred to an 80 °C oil bath and equipped with a condenser and stirring bar. 2-(4-aminophenyl)ethanol (2 g) and isoamyl nitrite (1.5 mL) was added. The mixture was stirred vigorously at 80 °C overnight. The mixture was centrifuged, and the supernatant was decanted away. The remaining solid material was washed with repeated cycles

of centrifugation and rinsing with DMF and deionized water. The final product was dried under vacuum at 40 °C.

Synthesis of rGO-DA-Br, rGO-DA-Br-blank, rGO-DA-PMMA and rGO-DA-PDEGA in batch reactor, rGO-DA-PMMA and rGO-DA-PDEGA in batch reactor at lower catalyst concentration and rGO-DA-PMMA and rGO-DA-PDEGA in flow reactor are the same as SI-photoCMP/1 approach.

Hydrolysis of PMMA from GO-PMMA samples.[14] 8 mg of KOH, 3 mL THF and 20 mg GO-PMMA were mixed, purged with nitrogen and placed to stir for 24 hours at 50 °C. The reaction mixture was quenched with methanol and filtered through a PTFE filter. The cleaved polymer was analyzed by SEC.

Results and Discussions

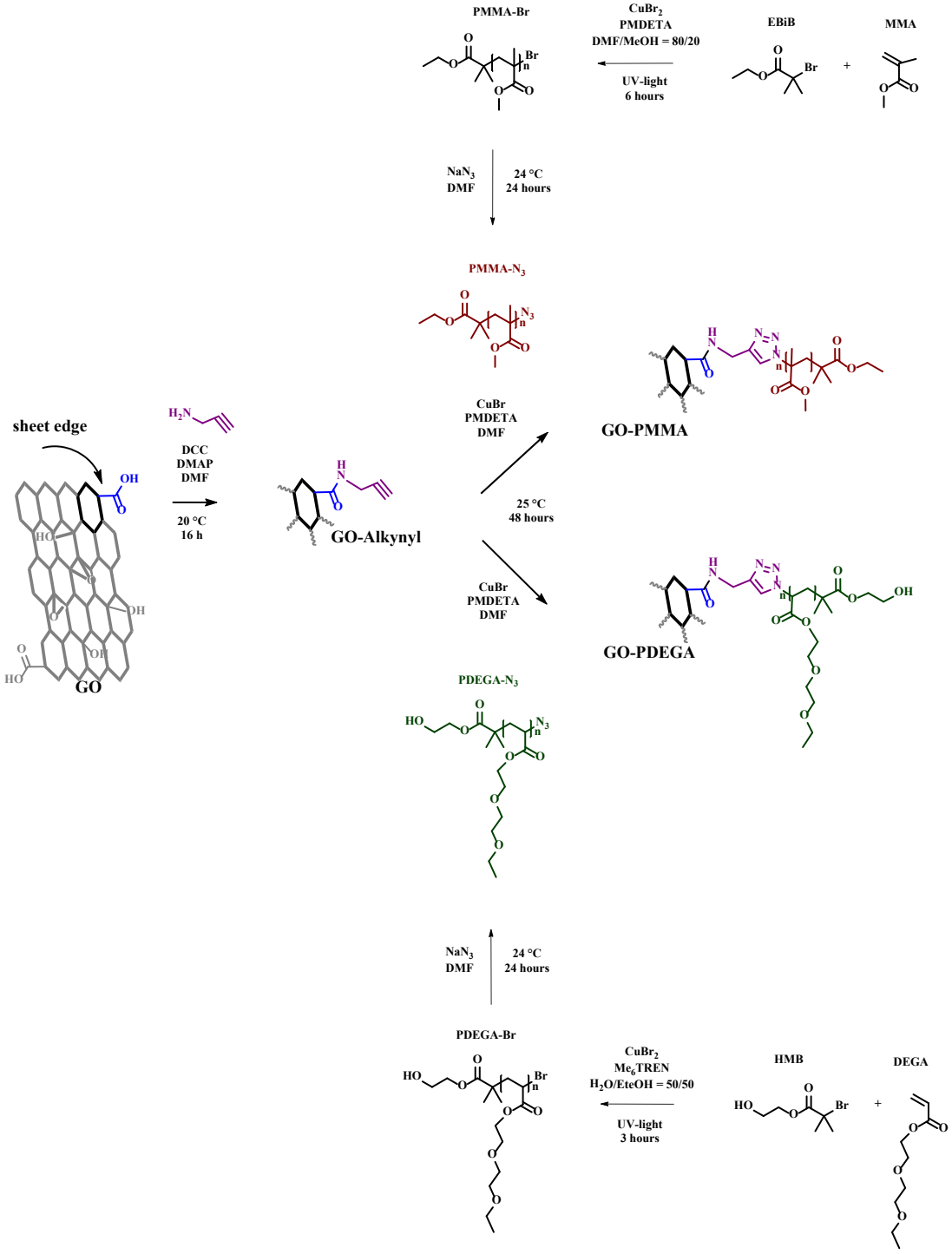

Scheme S1. A synthesis scheme of *grafting-to* method using the CuAAC approach.

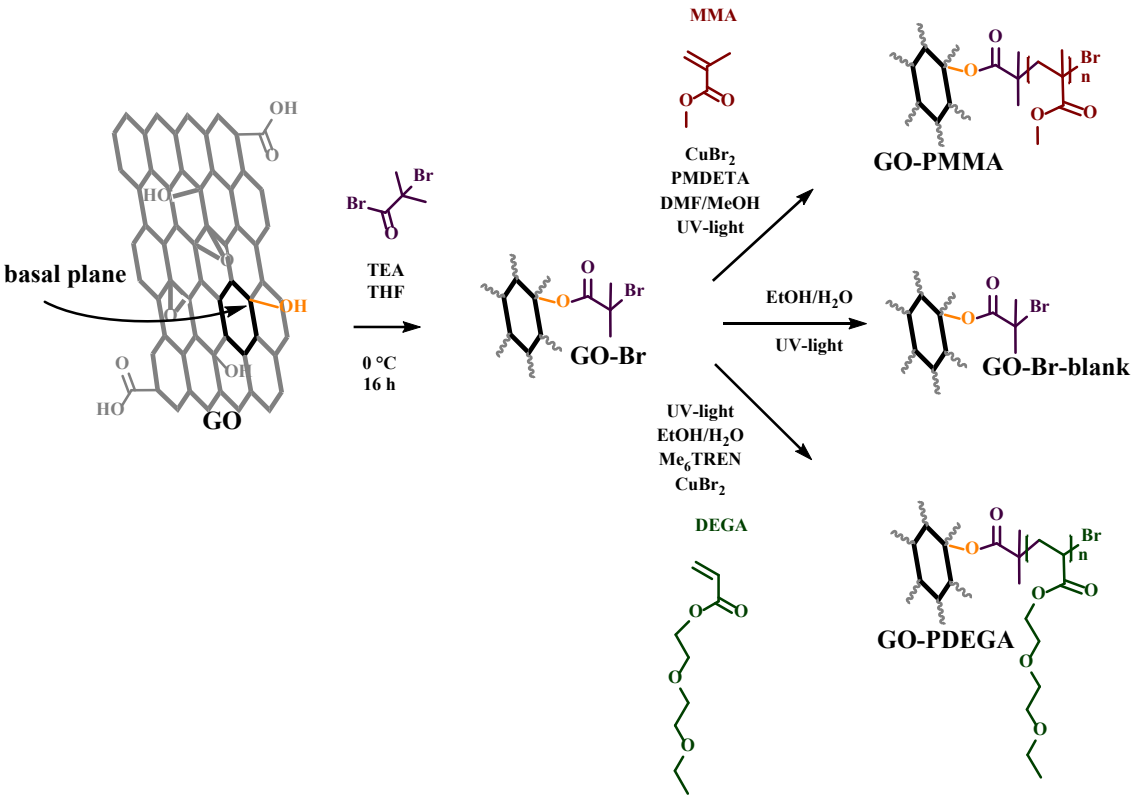

Scheme S2. A synthesis scheme of *grafting-from* method using the SI-photoCMP/1 approach.

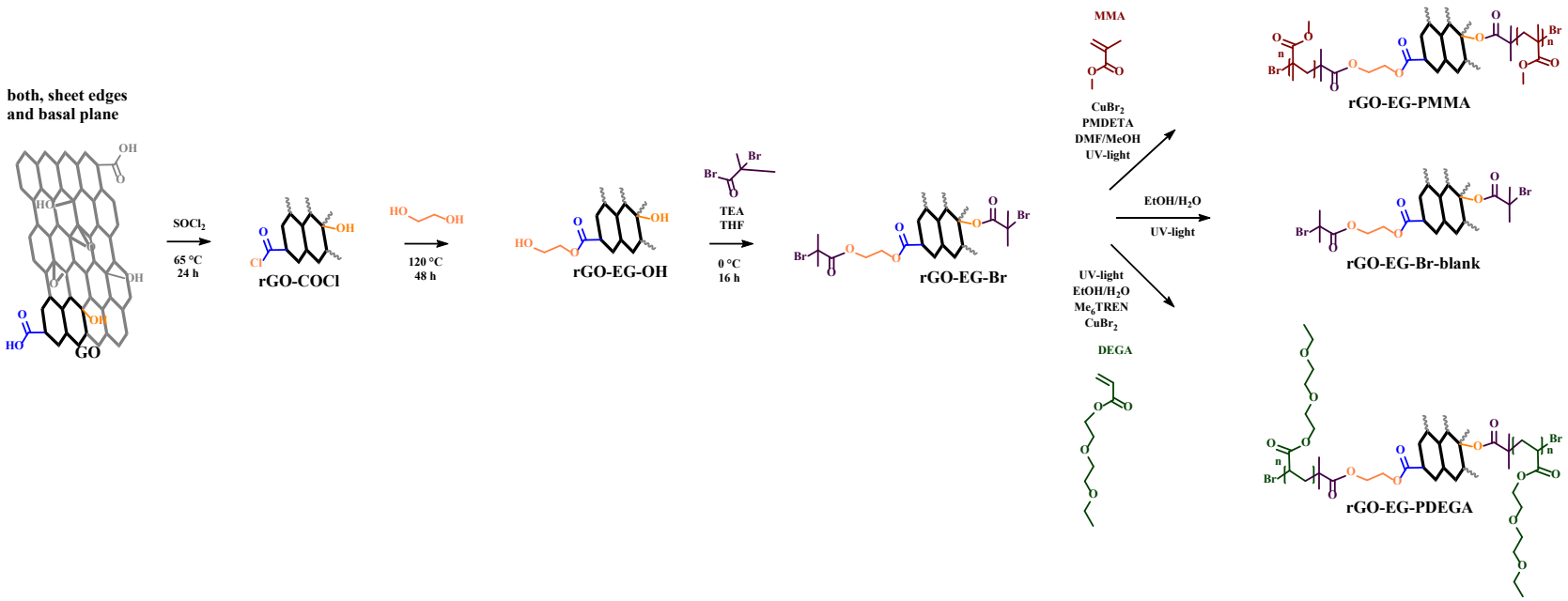

Scheme S3. A synthesis scheme of *grafting-from* method using the SI-photoCMP/2 approach.

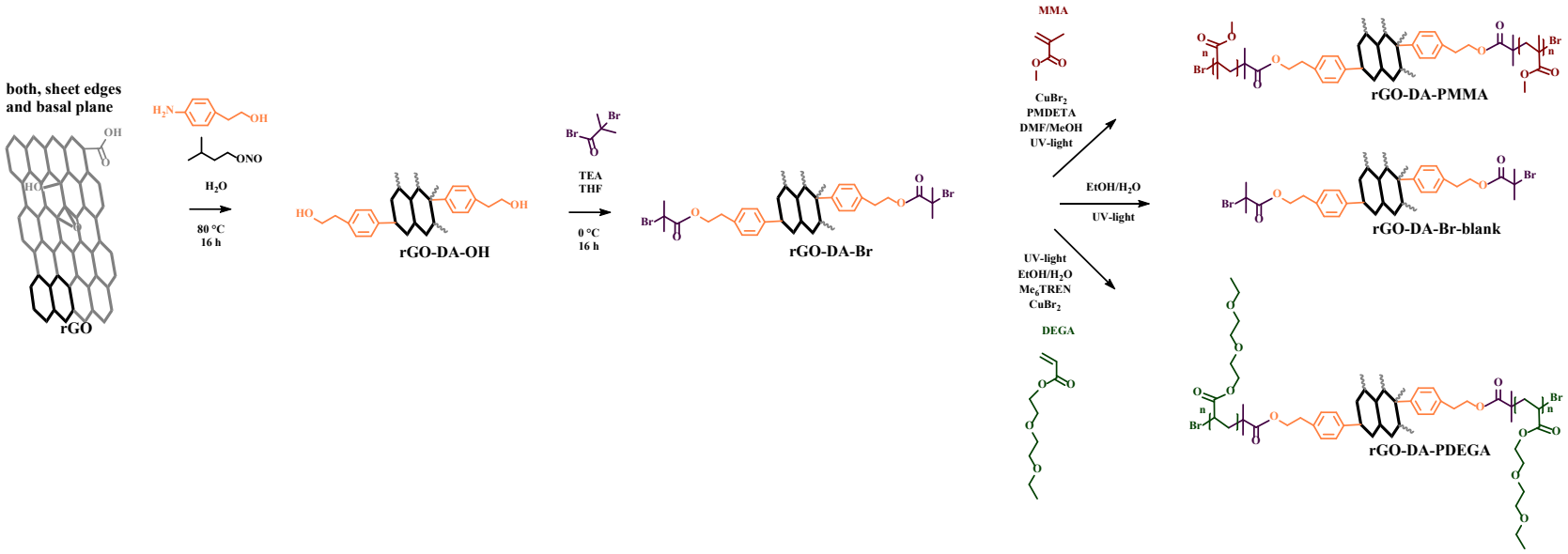

Scheme S4. A synthesis scheme of *grafting-from* method using the SI-photoCMP/3 approach.

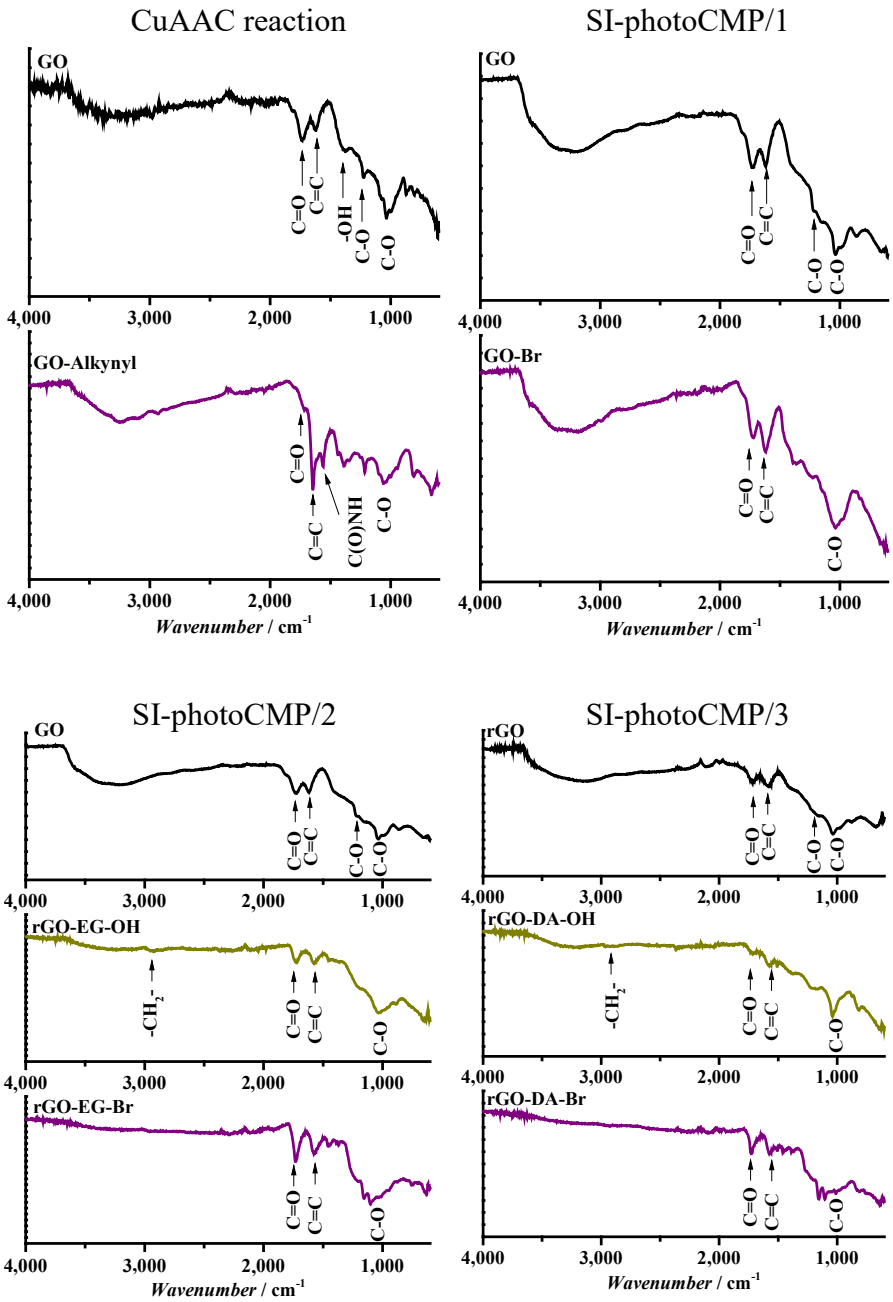

Figure S1. FT-IR spectra of GO/rGO-derivatives.

Solid-state ^{13}C NMR is a powerful analytical technique to analyze the structures of all GO/rGO-derivatives after each modification step. Solid-state ^{13}C NMR was used to distinguish between different carbon-oxygen functional groups of GO/rGO-derivatives (Figure S2). For the CuAAC technique, the spectra of GO, GO-Alkynyl, GO-PMMA/(M_n = 2,600 g/mol), and GO-PDEGA/(M_n = 2,700 g/mol) were analyzed and compared. The principal features of GO were assigned based on literature.[15] C(sp^2) resonances near 131 ppm, hydroxyl and epoxy groups at 70 ppm and 61 ppm respectively, lactol groups at 101 ppm, ketone near 190 ppm, ester and acids groups near 165 ppm. The 6-membered aromatic ring of the GO was used as a reference and the peak area of the C(sp^2) was integrated to be 6. As a result, the oxidation level of GO can be calculated *via* the ratio of hydroxyl and epoxy groups to C(sp^2)[7] and was obtained to be 2.5. GO-Alkynyl was synthesized after amidation between carboxyl groups of GO and amino groups of propargyl amine. According to the literature, carbon signals derived from the carbonyl groups showed resonances at 82.0 and 74.5 ppm which interferes with the signals of the hydroxyl and epoxy groups.[16] However, CH_2, located between the alkyne and the secondary amine groups was assigned at 30 ppm which is close to the literature result at 31.7 ppm. The new functional group R-C(O)-NH gives a resonance signal at 162 ppm. The presence of additional signals at 38, 105 and 156 ppm was attributed to traces of DMAP used during DCC coupling. Presumably, the presence of a hexagonal aromatic ring of DMAP interacts with the aromatic structure of GO *via* π-π stacking. Polymers were attached *via* an alkyne-azide cycloaddition reaction between alkyne groups of the GO-Alkynyl and azide groups of PMMA-N_3 and PDEGA-N_3 to yield a five-membered triazole ring. The carbon atoms of the triazole ring give resonance signals at 127 and 147 ppm and interfere with the C(sp^2) resonances of GO. In GO-PMMA/(2,600 g/mol) appearance of additional functionalities are attributed to PMMA and assigned to CH_3 at 16 ppm, the quaternary C and CH_2 backbone at 45

ppm, O-CH_3 at 52 ppm and R-C(O)-OR at 178 ppm.[17] In GO-PDEGA/(2,700 g/mol), signals of the PDEGA chains were assigned to CH_3 at 15 ppm, CH and CH_2 backbone at 41 ppm, O-CH_2 at 69 ppm and R-C(O)-OR at 174 ppm.

In the SI-photoCMP/1 the initiator, 2-bromoisobutyryl bromine was attached to the GO surface *via* an esterification reaction between hydroxyl groups of the GO and acyl bromide groups of the initiator. The solid-state ^{13}C NMR of GO-Br was not measured, however, the GO-Br-blank spectra is presented instead (Figure S2). The peak at 167 ppm was assigned to the R-C(O)-OR functionality. The C-Br signal was expected at 65.6 ppm and interferes with the C-OH and C-O-C signals of GO. Two CH_3 carbon atoms resonances were expected to be at 31 ppm, however, were not observed. According to the XPS results, the atomic percentage of Br was only 0.3% (Table S1). With the combination of the low presence of ^{13}C isotopes (1.1%) and low relative sensitivity of the ^{13}C NMR (0.016),[18] the initiator molecule was not detected. The small resonance peaks at 48 and 9 ppm could be assigned to traces of TEA. For GO-PMMA and GO-PDEGA, peak assignment is similar to GO-PMMA/(2,600 g/mol) and GO-PDEGA/(2,700 g/mol), respectively.

In SI-photoCMP/2, first, the carboxylic groups of GO were converted into acid chlorides in the presence of thionyl chloride for the formation of rGO-COCl. In a second step, the acid chloride groups are converted into ester functionalities *via* reaction with the hydroxyl groups of ethylene glycol to form rGO-EG-OH. The peak at 167 ppm assigned as R-C(O)-OR, CH_2 from EG can be assigned at 63.8 ppm, however, interferes with the C-OH and C-O-C resonances of GO. After the introduction of initiator molecule to the rGO surface, rGO-EG-Br is formed. The newly formed R-C(O)-OR functionality was assigned at 174 ppm, the resonance peak at 33 ppm attributed to CH_3 which is not far from their resonance in the liquid-state ^{13}C NMR at 31.0 ppm. The position of quaternary carbon atoms of the initiator is, according to liquid-state ^{13}C NMR, assigned at 65.6

ppm which again interferes with C-OH and C-O-C signals of GO. For rGO-EG-PMMA and rGO-EG-PDEGA, peak assignment is similar to GO-PMMA/(2,600 g/mol) and GO-PDEGA/(2,700 g/mol), respectively.

RGO with 0.90 oxidation level was used as a starting material in SI-photoCMP/3 while GO has 2.5. The signals can be assigned similar to the GO resonances. However, the peaks from the ketone and carbonyl carbons are absent. As a second step, a molecule of phenethyl alcohol was added and rGO-DA-OH was synthesized. The resonance signal of CH_2OH at 63.9 ppm, accordingly to liquid-state ^{13}C NMR interferes with C-OH and C-O-C signals of the GO. The appearance of the CH_2 signal at 35 ppm is close to the position according to liquid-state ^{13}C NMR at 38.3 ppm and proves the successful addition of the aryl derivative. The addition of initiator was proved *via* the presence of the signal at 172 ppm assigned to the R-C(O)-OR functionality. The signal at 33 ppm was attributed to CH_3 and interferes with the CH_2 resonances of the aryl derivative. The position of quaternary carbon form the initiator according to liquid-state ^{13}C NMR is at 65.6 ppm. For rGO-DA-PMMA and rGO-DA-PDEGA, peak assignment is similar to GO-PMMA/(2,600 g/mol) and GO-PDEGA/(2,700 g/mol) respectively.

In all cases the peak position of the GO-derivatives, attributed to $C(sp^2)$ broadened and shifted to a lower resonance frequency compare to bare GO. This can be explained by the variations of carbon atom environments after each modification step.[19]

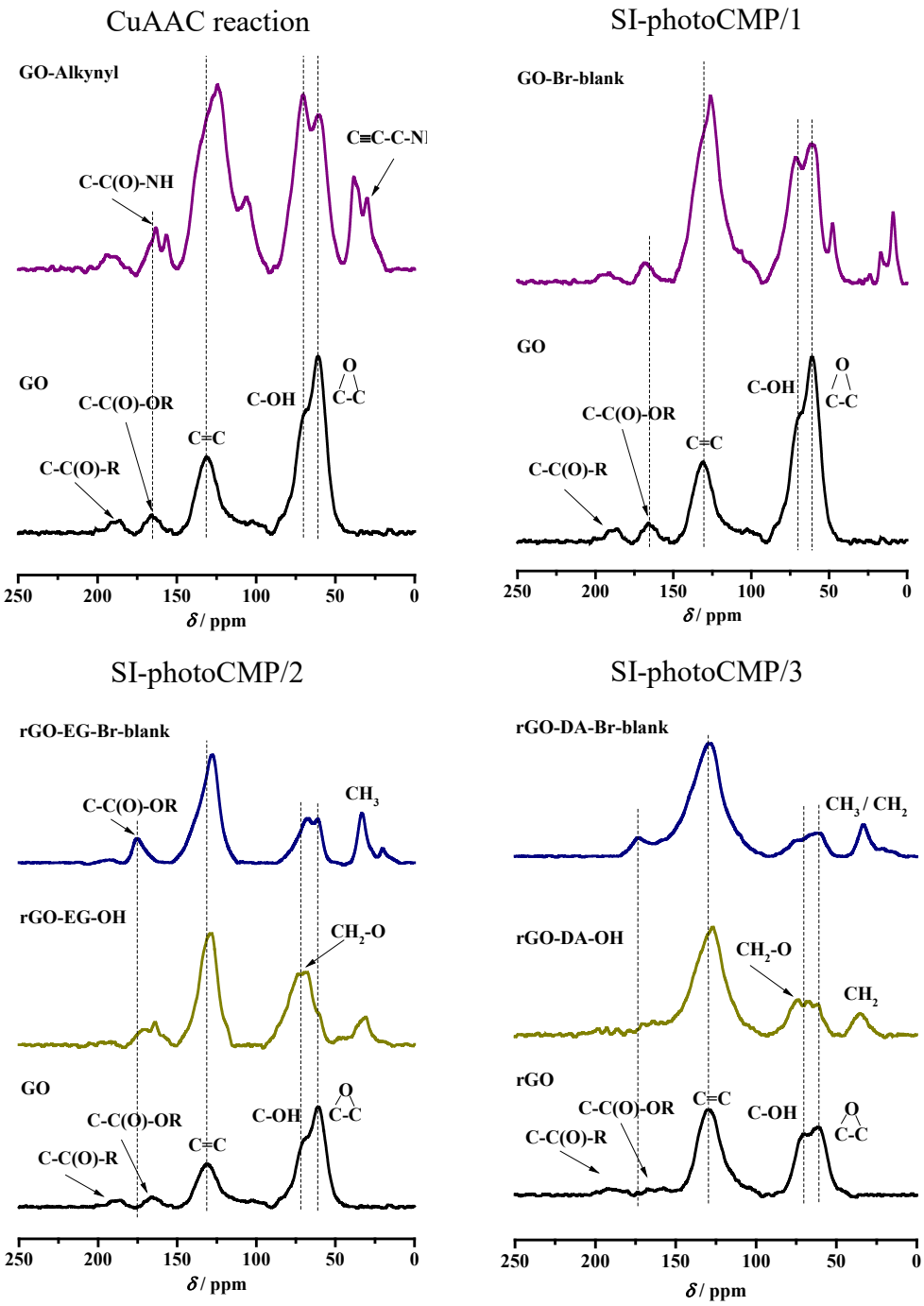

Figure S2. Solid-state ^{13}C NMR spectra of GO/rGO-derivatives.

Table S1. Concentration in atomic percentage of elements of GO-derivatives determined XPS.

GO-derivative	Br 3d	N 1s
CuAAC conjugation		
GO	-	0.4
GO-Alkynyl	-	5.1
GO-PMMA/(2,600 g/mol)	-	5.0
GO-PDEGA/(2,700 g/mol)	-	2.5
SI-photoCMP/1		
GO	-	0.4
GO-Br	0.3	0.9
GO-Br-blank	0.2	0.7
GO-PMMA	-	0.6
GO-PDEGA	-	1.0
SI-photoCMP/2		
GO	-	0.4
rGO-EG-OH	-	-
rGO-EG-Br	2.2	0.4
rGO-EG-Br-blank	1.8	0.3
rGO-EG-PMMA	-	-
rGO-EG-PDEGA	-	-
SI-photoCMP/3		
rGO	-	0.2
rGO-DA-OH	-	2.7
rGO-DA-Br	2.2	2.3
rGO-DA-Br-blank	1.7	2.0
rGO-DA-PMMA	-	-
rGO-DA-PDEGA	-	0.3

In general, detection limits for XPS range from 0.1 to 1 at%, depending on the elements.[20] Thus, low detected Br contents for SI-photoCMP/1 need to be read with care and should rather be

regarded as information towards the presence of covalently bound bromine. However, because of higher photoionization cross section, the detection limit for a heavy element (Br) in a light element matrix (graphene which is carbon-based) can reach 0.01 at.%, giving a possibility to compare the content of Br in all grafting-from systems. We can consider here the low concentration of Br as semi-quantitative. Concentrations of 0.3 and 2.2 at% are significantly different and not in the range of a possible error. These values can permit the evaluation of a modified graphene sample. To record as robust as possible data, we always measured samples at at least two different spots and over a 400 µm large excitation spot for each sample.

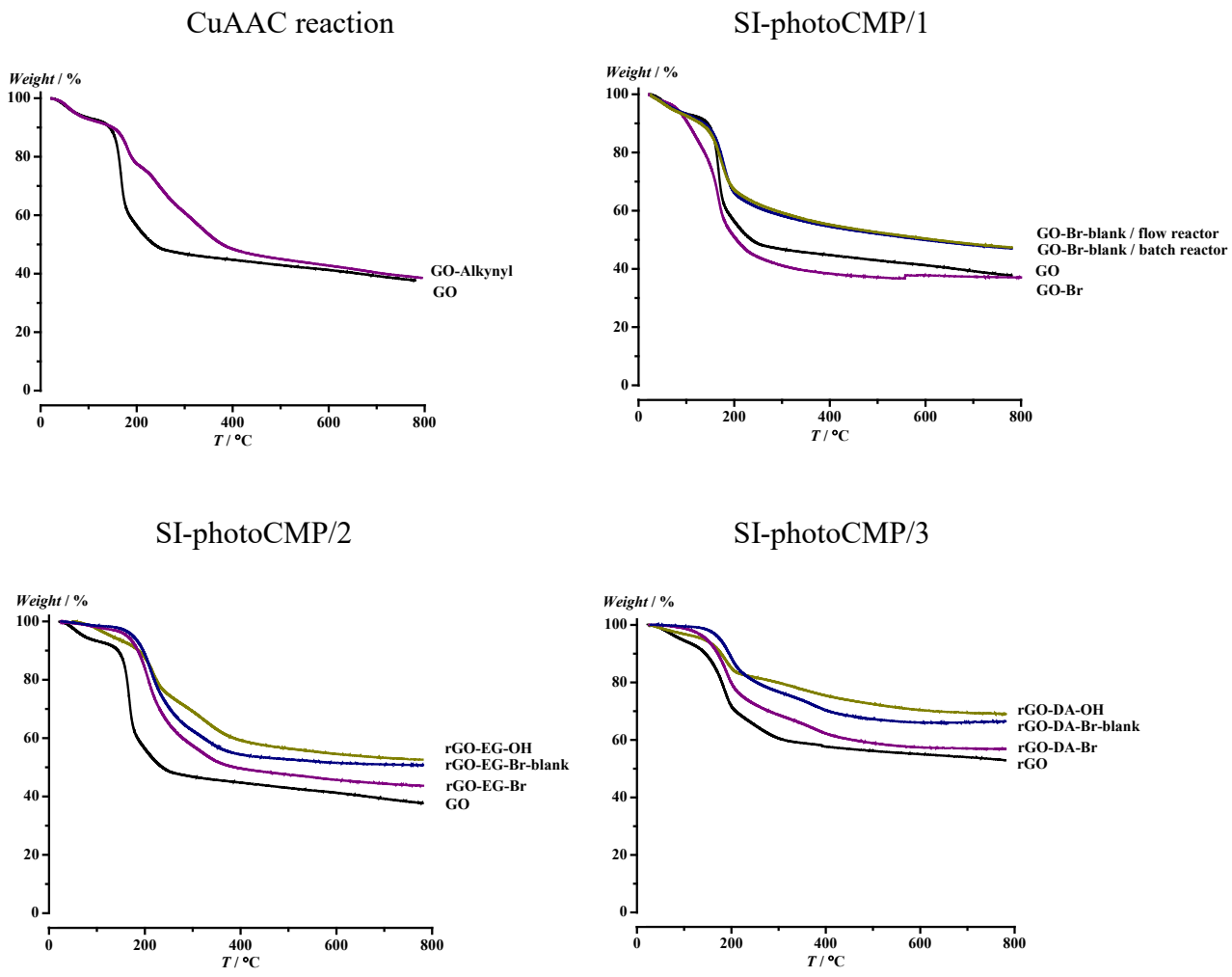

Figure S3. TGA thermograms of surface-functionalized GO/rGO.

Table S2. Summary table of obtained polymers.

DP	Conversion [%]	$M_{n,theor}$ [g/mol]	$M_{n,SEC}$ [g/mol]	Đ	$M_{n,SEC}$ [g/mol]	Đ
		PMMA-Br			**PMMA-N_3**	
25	48	1,300	2,600	1.33	2,600	1.34
100	47	4,800	7,100	1.32	7,100	1.32
		PDEGA-Br			**PDEGA-N_3**	
15	98	3,000	2,600	1.23	2,700	1.23
50	97	9,300	7,800	1.36	8,000	1.34

Table S3. Review table of synthesis conditions of CuAAC conjugation for GO-Alkynyl in DMF at room temperature for 48 hours.

polymer	$M_{n,SEC}$ [g/mol]	GO-Alkynyl : CuBr : PMDETA : polymer [mass ratio]
PMMA-N_3	2,600	0.1 : 0.528 : 0.638 : 2
PMMA-N_3	7,100	0.1 : 0.404 : 0.488 : 4
PDEGA-N_3	2,700	0.1 : 0.527 : 0.637 : 2
PDEGA-N_3	8,000	0.1 : 0.448 : 0.542 : 5

Table S4. Review table of synthesis conditions of SI-PhotoCMP.

GO-In.	Mon.	GO-Initiator : $CuBr_2$: Li [mass ratio]	Solvent ratio [vol%]	Reactor	Time [hours]
SI-photoCMP/1					
GO-Br	MMA	1 : 0.34 : 0.85	DMF/MeOH = 80/20	batch	24
		1 : 0.08 : 0.21		batch	24
		1 : 0.34 : 0.85		flow	1
	DEGA	1 : 0.24 : 1.5	EtOH/H_2O = 50/50	batch	24
		1 : 0.02 : 0.15		batch	24
		1 : 0.24 : 1.5		flow	1
SI-photoCMP/2					
rGO-EG-Br	MMA	1 : 0.34 : 0.85	DMF/MeOH = 80/20	batch	24
		1 : 0.08 : 0.21		batch	24
		1 : 0.34 : 0.85		flow	1
	DEGA	1 : 0.24 : 1.5	EtOH/H_2O = 50/50	batch	24
		1 : 0.02 : 0.15		batch	24
		1 : 0.24 : 1.5		flow	1
SI-photoCMP/3					
rGO-DA-Br	MMA	1 : 0.34 : 0.85	DMF/MeOH = 80/20	batch	24
		1 : 0.08 : 0.21		batch	24
		1 : 0.34 : 0.85		flow	1
	DEGA	1 : 0.24 : 1.5	EtOH/H_2O = 50/50	batch	24
		1 : 0.02 : 0.15		batch	24
		1 : 0.24 : 1.5		flow	1

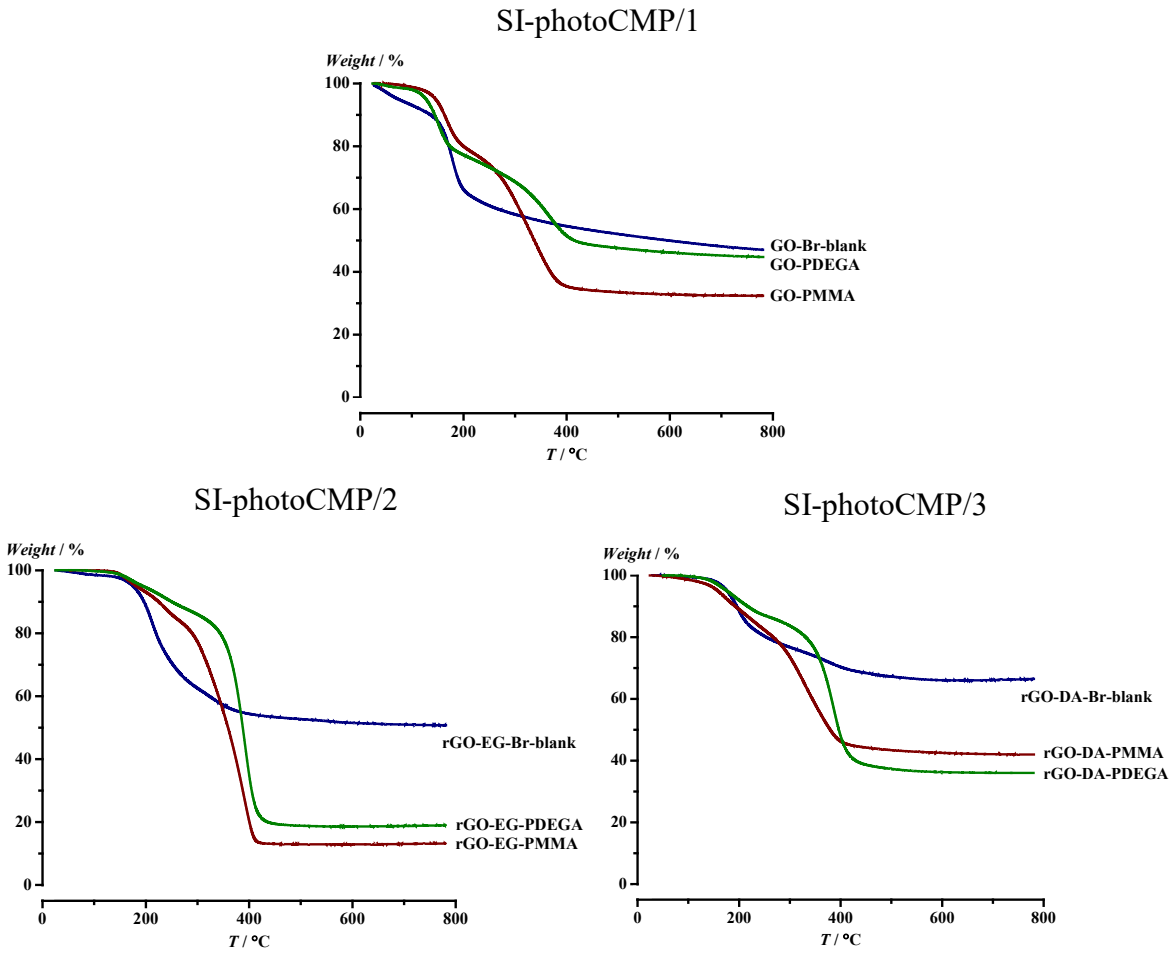

Figure S4. TGA thermograms of PMMA and PDEGA functionalized GO/rGO sheets *via* SI-photoCMP procedures.
Influence of reduced catalyst and ligand concentrations.
SI-PhotoCMP was carried out in UV-batch reactor at catalyst concentrations (0.75 mmol for MMA grafting and 0.54 mmol for DEGA grafting).
The polymer-grafted samples are compared to relevant blank samples.

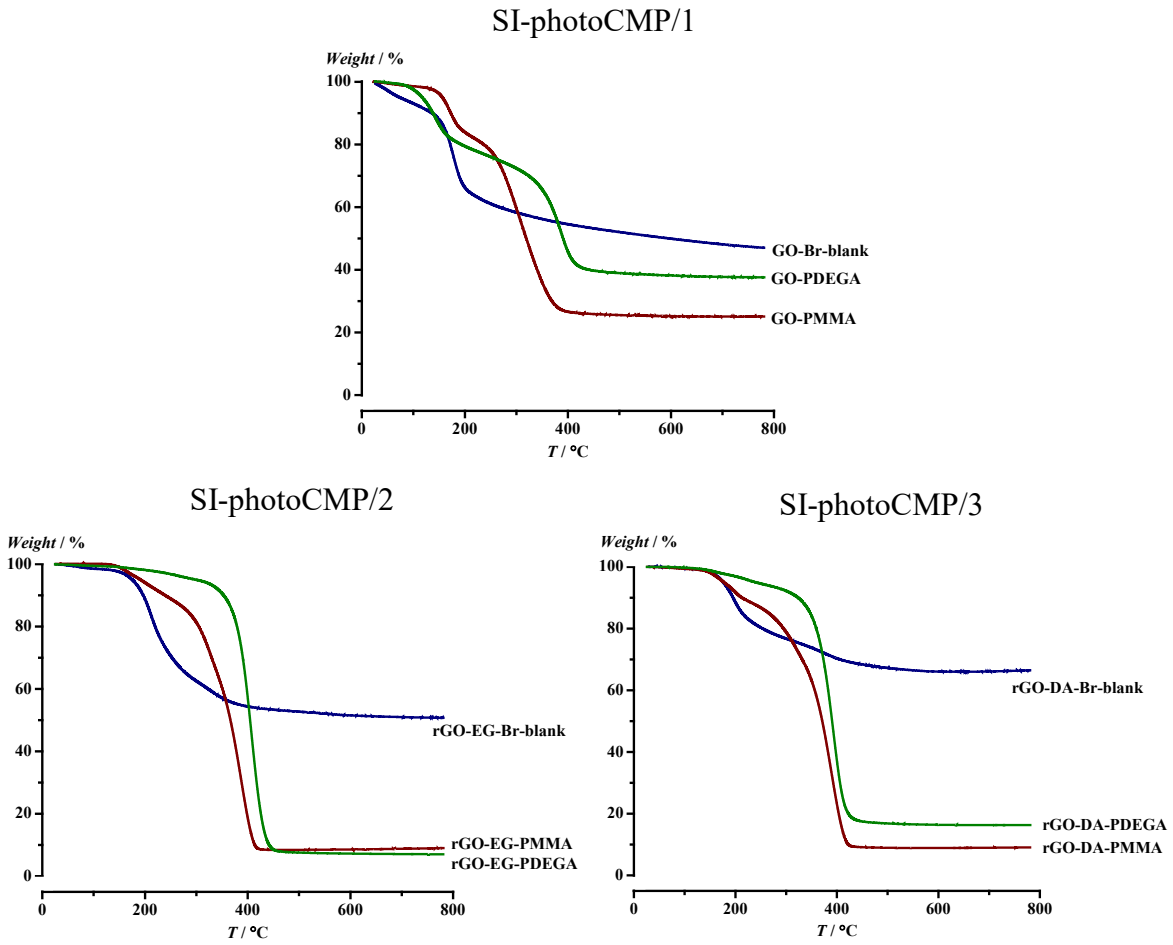

Figure S5. TGA thermograms of PMMA and PDEGA functionalized GO/rGO sheets *via* SI-photoCMP procedures.
SI-PhotoCMP was carried out in UV-flow reactor set-up.
The polymer-grafted samples are compared to relevant blank samples.

Figure S6. Flow reactor set up used for SI-photoCMP.

Calculation of functionalization density *via* TGA.

The calculation of grafting density is in detail shown for GO-PMMA sample, obtained using CuAAC reaction between GO-Alkynyl and PMMA with M_n = 2,600 g/mol

Calculation of the weight fractions of grafted PMMA, labile oxygen-containing groups (LOG) + linker between graphene surface and polymer chain, and graphene in GO-PMMA (M_n = 2,600 g/mol) sample.

$W(GO\text{-}PMMA) = W_{PMMA+LOG+linker}(GO\text{-}PMMA) + W_{graphene}(GO\text{-}PMMA)$,

100% = 57.3% + 42.7%

$W(GO\text{-}Alkynyl) = W_{LOG+linker}(GO\text{-}Alkynyl) + W_{graphene}(GO\text{-}Alkynyl)$,

100% = 47.9% + 52.1%

$W_{PMMA}(GO\text{-}PMMA) = W_{PMMA+LOG+linker}(GO\text{-}PMMA) - W_{LOG+linker}(GO\text{-}Alkynyl)$,

57.3% - 47.9% = 9.4%

$W_{LOG+linker}(GO\text{-}PMMA) = W_{PMMA+LOG+linker}(GO\text{-}PMMA) - W_{PMMA}(GO\text{-}PMMA)$,

57.3% - 9.4% = 47.9%

$W(GO\text{-}PMMA) = W_{PMMA}(GO\text{-}PMMA) + W_{LOG+linker}(GO\text{-}PMMA) + W_{graphene}(GO\text{-}PMMA)$,

100% = 9.4% + 47.9% + 42.7%

where $W_{PMMA}(GO\text{-}PMMA)$, $W_{LOG+linker}(GO\text{-}PMMA)$, $W_{graphene}(GO\text{-}PMMA)$ are the weight fractions of PMMA, labile oxygen-containing functional groups (LOG) + linker between graphene surface and polymer chain, and graphene in GO-PMMA.

$W_{LOG+linker}(GO\text{-}Alkynyl)$, $W_{graphene}(GO\text{-}Alkynyl)$ are the weight fractions of LOG + linker and graphene in GO-Alkynyl.

The weight fractions are obtained from the TGA curves at 600 °C and represented in percent.

Calculation of the weight ratios of grafted PMMA and GO-Alkynyl.

$$\mathbf{WR_{PMMA}(GO\text{-}PMMA)} = \frac{W_{\mathbf{PMMA}}(\mathbf{GO-PMMA})}{(W_{\mathbf{PMMA}}(\mathbf{GO-PMMA}) + W_{\mathbf{LOG+linker}}(\mathbf{GO-PMMA}) + W_{\mathbf{graphene}}(\mathbf{GO-PMMA}))} \times \mathbf{100}\%$$

$$= \frac{9.4}{(9.4 + 47.9 + 42.7)} \times 100\% = 9.4\%$$

$$\mathbf{WR_{GO\text{-}Alkynyl}(GO\text{-}PMMA)} = \frac{(W_{\mathbf{LOG+linker}}(\mathbf{GO-PMMA}) + W_{\mathbf{graphene}}(\mathbf{GO-PMMA}))}{(W_{\mathbf{PMMA}}(\mathbf{GO-PMMA}) + W_{\mathbf{LOG+linker}}(\mathbf{GO-PMMA}) + W_{\mathbf{graphene}}(\mathbf{GO-PMMA}))} \times \mathbf{100}\% =$$

$$\frac{(47.9 + 42.7)}{(9.4 + 47.9 + 42.7)} \times 100\% = 90.6\%$$

where WR_{PMMA}(GO-PMMA) and $WR_{GO\text{-}Alkynyl}$(GO-PMMA) are the weight ratios of PMMA and GO-Alkynyl respectively.

Calculation of the weight ratios of grafted PMMA and graphene.

$$\mathbf{WR_{PMMA}(GO\text{-}PMMA)} = \frac{W_{\mathbf{PMMA}}(\mathbf{GO-PMMA})}{(W_{\mathbf{PMMA}}(\mathbf{GO-PMMA}) + W_{\mathbf{graphene}}(\mathbf{GO-PMMA}))} \times \mathbf{100}\% = \frac{9.4}{(9.4 + 42.7)} \times 100\%$$

$$= 18.0\%$$

$$\mathbf{WR_{C}(GO\text{-}PMMA)} = \frac{W_{\mathbf{graphene}}(\mathbf{GO-PMMA})}{(W_{\mathbf{PMMA}}(\mathbf{GO-PMMA}) + W_{\mathbf{graphene}}(\mathbf{GO-PMMA}))} \times \mathbf{100}\% = \frac{42.7}{(9.4 + 42.7)} \times 100\%$$

$$= 82.0\%$$

where WR_{PMMA}(GO-PMMA) and WR_{C}(GO-PMMA) are the weight ratios of PMMA and graphene respectively.

Calculation of pMMA grafting to 1 g of graphene.

$$\mathbf{m(PMMA)} = \frac{\frac{WR_{\mathbf{PMMA}}(\mathbf{GO-PMMA})}{100\ \%}}{\frac{WR_{C}(\mathbf{GO-PMMA})}{100\ \%}} = \frac{0.18}{0.82} = 0.219\ \text{g}$$

where m(PMMA) is the mass of PMMA per gram of graphene.

Calculation of polymer grafting density.

 # PMMA chains per gram of graphene = ν · N_A = $\frac{m(PMMA) \times N_A}{Mn(PMMA)} = \frac{0.219 \times 6.022 \times 10^{23}}{2{,}600} =$

$= 5.07 \times 10^{19}$

where N_A is Avogadro constant and equals 6.022×10^{23} mol^{-1}, m(PMMA) is the mass of PMMA per gram of graphene, M_n(PMMA) is the molecular weight of PMMA = 2,600 g/mol, obtained from SEC, and ν is the # moles of PMMA.

 # moles of PMMA per # moles of graphene = $\frac{\nu(\text{PMMA})}{\nu(\text{C})} = \frac{m(\text{PMMA}) \times Ar(C)}{Mn(\text{PMMA}) \times m(C)} = \frac{0.219 \times 12}{2{,}600 \times 1} = 0.00101$

where ν(PMMA) and ν(C) are the # moles of PMMA and graphene, respectively, m(PMMA) is the mass of PMMA per gram of graphene, M_n(PMMA) is the molecular weight of PMMA = 2,600 g/mol, obtained from SEC, A_r(C) is the relative atomic mass of carbon (A_r(C) = 12 g/mol) and m(C) is the mass of graphene in gram.

 # PMMA chains per 10,000 carbons of graphene = $\frac{\nu(PMMA) \times N_A}{\nu(\text{C}) \times N_A} \times 10{,}000 = 10.10$

 # carbons of graphene per grafted PMMA chain = $\frac{1 \times 10{,}000}{\#\text{ of } PMMA \text{ chains per } 10{,}000 \text{ carbons of graphene}} = 990$

 # PMMA chains per nm² graphene = $\frac{\#\text{ carbons per aromatic ring of graphene}}{\#\text{ carbons of graphene with one grafted } PMMA \text{ chain} \times Å^2}$

where # carbons per aromatic ring of graphene is 6, number of graphene carbons per grafted PMMA chain is 990, and $Å^2$ is the area of a benzene ring in graphene (0.0524 nm^2).

Table S5. Summarized content of the samples, obtained from TGA, determined from the weight loss at 600 °C.

sample	reactor	Composition [wt%]		
		PMMA	**PMMA**	**PMMA**
GO-PMMA/ (2,600 g/mol)	batch	9.4	9.4	9.4
GO-PMMA/ (7,100 g/mol)	batch	8.0	8.0	8.0
GO-PMMA	batch	29.6	29.6	29.6
	flow	24.7	24.7	24.7
	batch; 1.88 mmol of Cat.	17.1	17.1	17.1
rGO-EG-PMMA	batch	49.5	49.5	49.5
	flow	42.9	42.9	42.9
	batch; 1.88 mmol of Cat.	38.6	38.6	38.6
rGO-DA-PMMA	batch	60.1	60.1	60.1
	flow	57.2	57.2	57.2
	batch; 1.88 mmol of Cat.	23.5	23.5	23.5
sample	**reactor**	**PDEGA**	**PDEGA**	**PDEGA**
GO-PDEGA/ (2,700 g/mol)	batch	18.7	18.7	18.7
GO-PDEGA/ (8,000 g/mol)	batch	11.6	11.6	11.6
GO-PDEGA	batch	23.5	23.5	23.5
	flow	11.8	11.8	11.8
	batch; 0.54 mmol of Cat.	3.8	3.8	3.8
rGO-EG-PDEGA	batch	45.8	45.8	45.8
	flow	44.3	44.3	44.3
	batch; 0.54 mmol of Cat.	32.9	32.9	32.9
rGO-DA-PDEGA	batch	50.6	50.6	50.6
	flow	49.7	49.7	49.7
	batch; 0.54 mmol of Cat.	29.8	29.8	29.8

Table S6. Summarized grafting ratios, obtained from TGA, determined from the weight loss at 600 °C.

sample	reactor	Grafting ratio [wt%]		Grafting ratio [wt%]	
		PMMA	GO-deriv.	PMMA	graphene
GO-PMMA/ (2,600 g/mol)	batch	9.4	90.6	18.0	82.0
GO-PMMA/ (7,100 g/mol)	batch	8.0	92.0	15.4	84.6
GO-PMMA	batch	29.6	70.4	59.2	40.8
	flow	24.7	75.3	49.5	50.5
	batch; 1.88 mmol of Cat.	17.1	82.9	34.2	65.8
rGO-EG-PMMA	batch	49.5	50.5	96.0	4.0
	flow	42.9	57.1	83.3	16.7
	batch; 1.88 mmol of Cat.	38.6	61.4	74.9	25.1
rGO-DA-PMMA	batch	60.1	39.9	91.0	9.0
	flow	57.2	42.8	86.5	13.5
	batch; 1.88 mmol of Cat.	23.5	76.5	35.6	64.4
sample	**reactor**	**PDEGA**	**GO-deriv.**	**PDEGA**	**graphene**
GO-PDEGA/ (2,700 g/mol)	batch	18.7	81.3	35.8	64.2
GO-PDEGA/ (8,000 g/mol)	batch	11.6	88.4	22.3	77.7
GO-PDEGA	batch	23.5	76.5	47.1	52.9
	flow	11.8	88.2	23.5	76.5
	batch; 0.54 mmol of Cat.	3.8	96.2	7.6	92.4
rGO-EG-PDEGA	batch	45.8	54.2	88.9	11.1
	flow	44.3	55.7	85.9	14.1
	batch; 0.54 mmol of Cat.	32.9	67.1	63.9	36.1
rGO-DA-PDEGA	batch	50.6	49.4	76.5	23.5
	flow	49.7	50.3	75.1	24.9
	batch; 0.54 mmol of Cat.	29.8	70.2	45.1	54.9

Table S7. Comparison of PMMA and PDEGA grafting using CuAAC coupling, obtained from TGA. Results represented as polymer grafting (in grams) to 1 gram of graphene.

sample	**PMMA grafting (grams) to 1 gram of graphene**
GO-PMMA/(2,600 g/mol)	0.22
GO-PMMA/(7,100 g/mol)	0.18
	PDEGA grafting (grams) to 1 gram of graphene
GO-PDEGA/(2,700 g/mol)	0.56
GO-PDEGA/(8,000 g/mol)	0.29

In Figure S7, FT-IR spectra give the signals for both attached PMMA and PDEGA. The C-H stretching mode vibrations at 2,964 and 2,873 cm^{-1}, the C=O vibration at 1,734 cm^{-1}, the C-H bending at 1,450 cm^{-1} and the backbone stretching mode of $(CH_2)_n$ at 980 cm^{-1}, 835 cm^{-1}, and 744 cm^{-1} were observed. Additionally, the intensive C-O stretching mode was observed at 1,149 cm^{-1} (PMMA) and at 1,109 cm^{-1} (PDEGA).

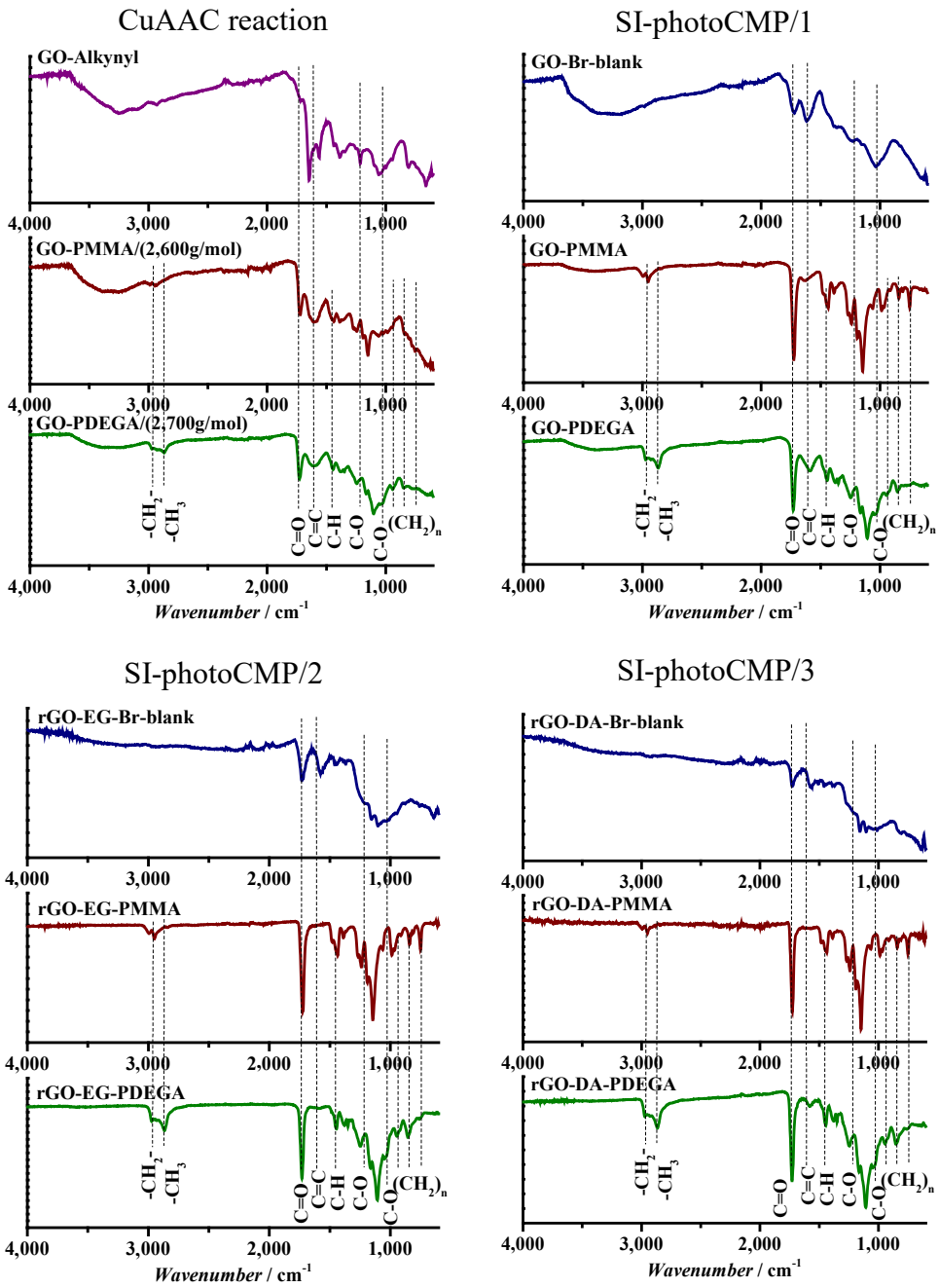

Figure S7. FT-IR spectra of PMMA and PDEGA functionalized GO/rGO sheets *via* CuAAC reaction and SI-photoCMP procedures. The samples compared to relevant blank samples.

Table S8. XPS: atomic ratios of the different C 1s components of GO-derivatives. Comparison with theoretical carbon environment of MMA and DEGA.

	C1s		
GO-derivative	**C-C, C-H**	**C-O**	**O=C-O**
PMMA (theoretical values)	*3.0*	*1.0*	*1.0*
GO-PMMA/(2,600 g/mol)	4.0	3.5	1.0
GO-PMMA	3.2	1.5	1.0
rGO-EG-PMMA	3.1	1.2	1.0
rGO-DA-PMMA	3.2	1.3	1.0
PDEGA (theoretical values)	*3.0*	*5.0*	*1.0*
GO-PDEGA/(2,700 g/mol)	3.6	4.6	1.0
GO-PDEGA	3.2	4.8	1.0
rGO-EG-PDEGA	2.7	4.7	1.0
rGO-DA-PDEGA	3.7	4.6	1.0

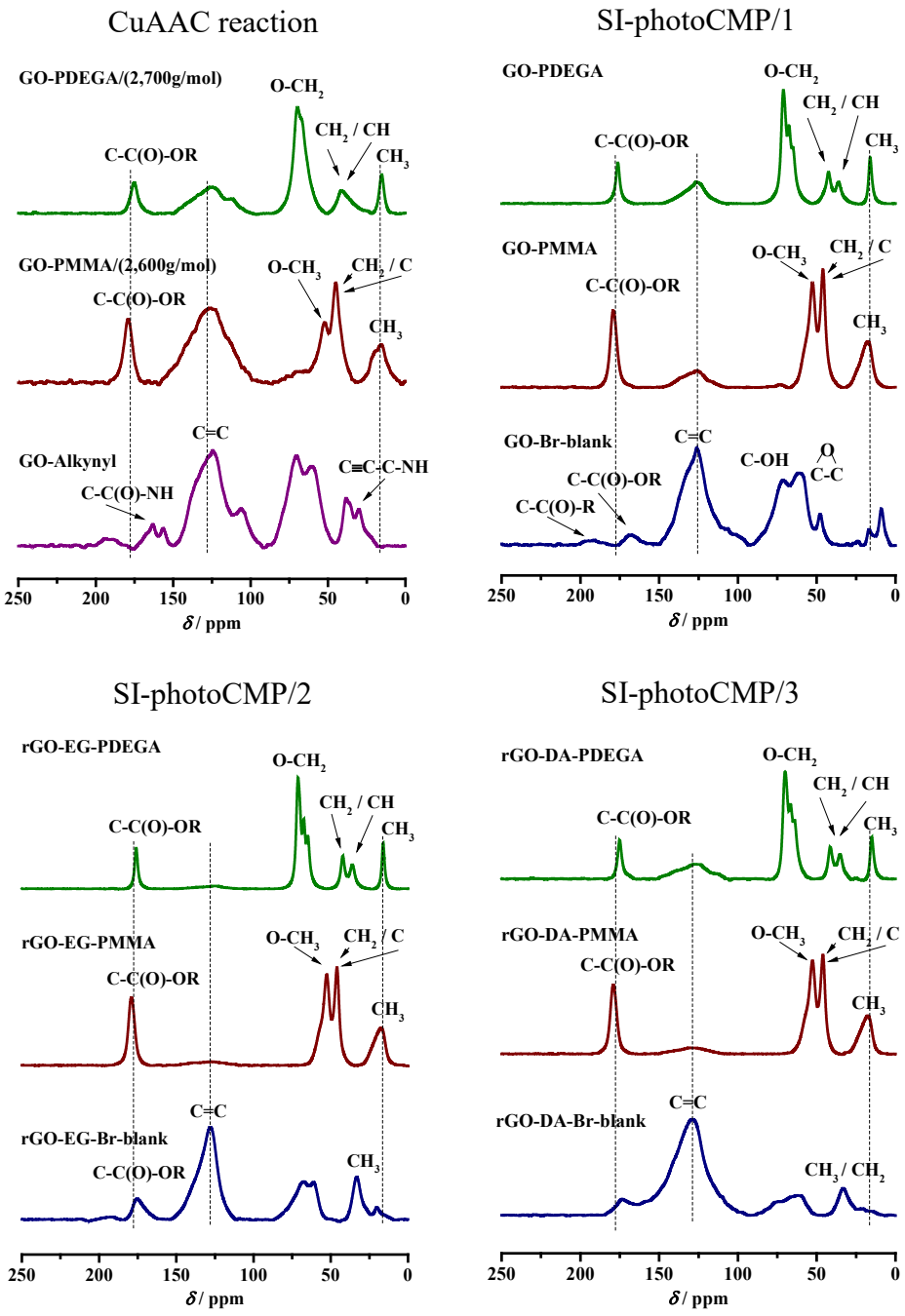

Figure S8. Solid-state ^{13}C NMR of PMMA and PDEGA functionalized GO/rGO sheets *via* CuAAC reaction and SI-photoCMP procedures.
The samples compared to relevant blank samples.

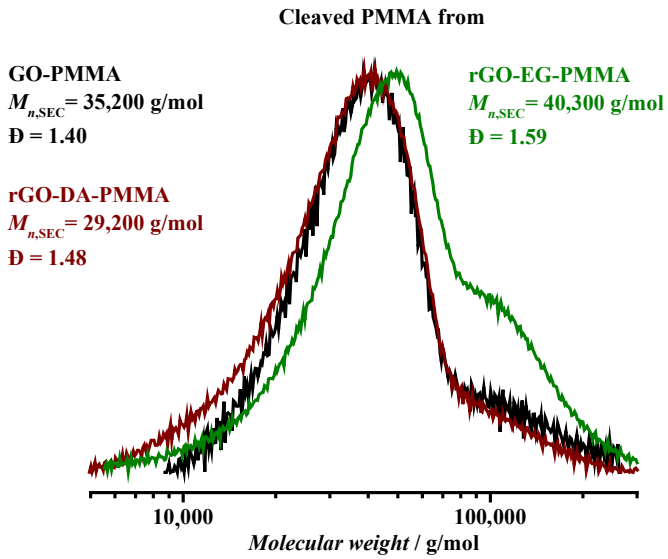

Figure S9. SEC analysis of cleaved PMMA from GO-PMMA, rGO-EG-PMMA and rGO-DA-PMMA, obtained *via* SI-PhotoCMP in a UV-batch reactor at 7.5 mmol catalyst concentration.

Control over polymer absorption to bare GO surface.

The experiment was designed towards investigating the absorption of polymer chains (PMMA and PDEGA) to GO sheet surface and the following control towards removing of absorbed polymer chains *via* filtration and washing with an excess of different solvents. The ToF-SIMS was recorded and compared to GO-PMMA/(M_n = 2,600 g/mol) and GO-PDEGA/(M_n = 2,700 g/mol) samples.

1) **Bare GO** (0.1 g), **PMMA-N_3** (2.0 g, 1 eq.) and PMDETA (0.638 g, 5 eq.) were loaded into a 50 mL Schlenk flask, dissolved in DMF (30 mL) and degassed four times by freeze-vacuum-thaw cycles. CuBr (0.528 g, 5 eq.), was added in the presence of argon atmosphere. The mixture was stirred for 48 h at room temperature. The obtained product called **GO/PMMA-control** was filtered through a RC membrane with pore size 0.45 μm and washed with an excess of THF, EtOH and distilled water and then dried under vacuum at 40 °C.

2) **Bare GO** (0.1 g), **PDEGA-N_3** (2.0 g, 1 eq.) and PMDETA (0.637 g, 5 eq.) were charged into a 50 mL Schlenk flask, dissolved in DMF (30 mL) and degassed four times by freeze-vacuum-thaw cycles. CuBr (0.527 g, 5 eq.), was added in the presence of argon atmosphere. The mixture was stirred for 48 h at room temperature. The obtained product called **GO/PDEGA-control**, was filtered through a RC membrane with pore size 0.45 μm and washed with an excess of THF, EtOH and distilled water and then dried under vacuum at 40 °C.

For both samples, GO-PMMA/(M_n = 2,600 g/mol) and GO/PMMA-control, the intensity of $C_4H_5O_2^-$ fragments were compared. In GO-PMMA/(M_n = 2,600 g/mol), the PMMA chains were covalently attached using CuAAC conjugation. The presence of an intensive signal of $C_4H_5O_2^-$ fragment of GO-PMMA/(M_n = 2,600 g/mol) and absence of the signal of GO/PMMA-control sample was observed.

The similar results were obtained for GO-PDEGA/(M_n = 2,700 g/mol) and GO/PDEGA-control samples. The intensive signal of $C_2H_3O^-$ fragment was observed for GO-PDEGA/(2,700g/mol) sample and no signal for GO/PDEGA-control sample.

As result, the successful removal of absorbed PMMA and PDEGA chains from GO was obtained *via* filtration and washing with an excess of different solvents, assessed *via* ToF-SIMS.

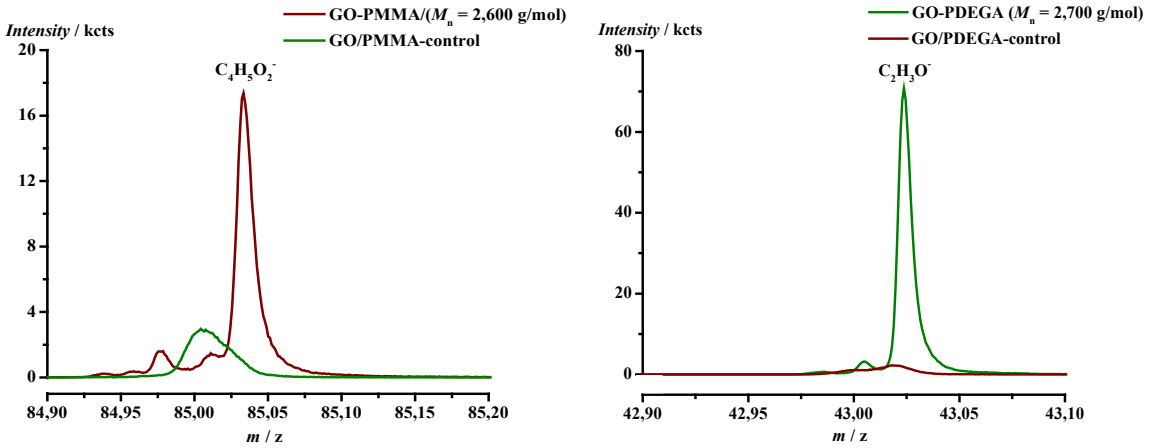

Figure S10. ToF-SIMS spectra of $C_4H_5O_2^-$ and $C_2H_3O^-$ fragments.

We have made sure that wherever suitable assignments for the mass spectra signals were given in the text. These assignments, like $C_2H_3O^-$ and $C_4H_5O_2^-$, are verified by several means; their exact mass, their $^{12}C/^{13}C$ isotopic pattern (especially for larger fragments) and cross validations with SIMS libraries. Apart from own measurements on reference polymers, the most important library used is provided from IONTOF GmbH, Münster, Germany, based on polymer obtained from Polymer Standards Service GmbH (PSS), Mainz, Germany. It is very important to note here that the SIMS characterization is of course not solely based on ONE signal for each modification as shown in Figs. 6 and 7. In fact a whole set of peaks from the recorded mass spectra was used for S40

the characterization of both modifications. These were for the MMA system: CH_3O, $C_4H_5O_2$ as shown, $C_5H_5O_2$, $C_5H_9O_2$, C_6H_7O, C_7H_7O, C_7H_9O, $C_7H_7O_3$, $C_7H_9O_2$, and $C_9H_{13}O_4$ in negative secondary ion polarity; and $C_5H_9O_2$, C_6H_9O, $C_5H_{10}O_2$, C_7H_9O, $C_6H_7O_2$, $C_6H_{11}O_2$, $C_7H_{10}O_2$, $C_6H_7O_3$, $C_7H_{11}O_2$, $C_8H_{14}O_2$, and $C_9H_{14}O_4$ in positive SI polarity. For the EG system C_2HO, C_2H_3O as shown in Fig. 7, $C_2H_2O_2$, $C_2H_3O_2$, C_2H_5O, $C_2H_5O_2$, C_2HO_2, C_4H_3O, $C_3H_3O_2$, and $C_4H_7O_2$ in negative Si polarity; as well as CH_3O, C_2H_4O, C_2H_5O, $C_4H_7O_2$, $C_5H_7O_2$, $C_5H_{11}O_2$, and $C_6H_{13}O_2$ in positive SI are characteristic of this modification.

Moreover, several spots on the samples were analyzed to provide a better overview. Samples were spotted GO suspensions on Si wafers, dried, leaving behind a random arrangement of GO particles varying in local particle density across the spots. This introduces some variation in the signal intensities in the range of ± 10%.

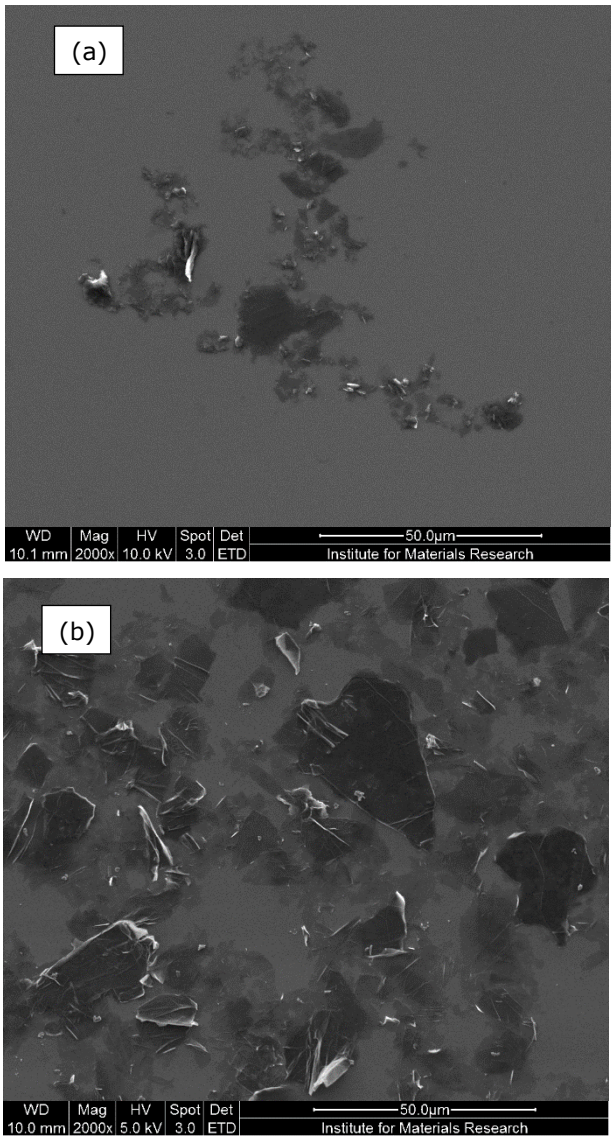

Figure S11. SEM micrographs of the GO used. Top (a) shows lab-synthesized GO and the bottom (b) gives commercially sourced rGO

References

[1] L. Feng, J. W. Hu, Z. L. Liu, F. B. Zhao, G. J. Liu, *Polymer* **2007**, *48*, 3616-3623.

[2] Z. Yin, C. Koulic, C. Pagnoulle, R. Jérôme, *Macromolecules* **2001**, *34*, 5132-5139.

[3] K. L. Parry, A. Shard, R. Short, R. White, J. Whittle, A. Wright, *Surface and Interface Analysis: An International Journal devoted to the development and application of techniques for the analysis of surfaces, interfaces and thin films* **2006**, *38*, 1497-1504.

[4] J. H. Scofield, *Journal of Electron Spectroscopy and Related Phenomena* **1976**, *8*, 129-137.

[5] Y.-J. Chen, J. Li, N. Hadjichristidis, J. W. Mays, *Polymer Bulletin* **1993**, *30*, 575-578.

[6] B. Appelt, G. Meyerhoff, *Macromolecules* **1980**, *13*, 657-662.

[7] D. C. Marcano, D. V. Kosynkin, J. M. Berlin, A. Sinitskii, Z. Sun, A. Slesarev, L. B. Alemany, W. Lu, J. M. Tour, *ACS Nano* **2010**, *4*, 4806-4814.

[8] Y. Pan, H. Bao, N. G. Sahoo, T. Wu, L. Li, *Advanced Functional Materials* **2011**, *21*, 2754-2763.

[9] Y.-M. Chuang, B. Wenn, S. Gielen, A. Ethirajan, T. Junkers, *Polymer Chemistry* **2015**, *6*, 6488-6497.

[10] S. Railian, B. Wenn, T. Junkers, *Journal of Flow Chemistry* **2016**, *6*, 260-267.

[11] M. Peeters, S. Kobben, K. Jiménez-Monroy, L. Modesto, M. Kraus, T. Vandenryt, A. Gaulke, B. van Grinsven, S. Ingebrandt, T. Junkers, *Sensors and Actuators B: Chemical* **2014**, *203*, 527-535.

[12] G. Goncalves, P. A. A. P. Marques, A. Barros-Timmons, I. Bdkin, M. K. Singh, N. Emami, J. Gracio, *Journal of Materials Chemistry* **2010**, *20*, 9927-9934.

[13] M. Fang, K. Wang, H. Lu, Y. Yang, S. Nutt, *Journal of Materials Chemistry* **2009**, *19*, 7098-7105.

[14] D. Baskaran, J. W. Mays, M. S. Bratcher, *Angewandte Chemie* **2004**, *116*, 2190-2194.

[15] aA. Lerf, H. He, M. Forster, J. Klinowski, *The Journal of Physical Chemistry B* **1998**, *102*, 4477-4482; bW. Gao, L. B. Alemany, L. Ci, P. M. Ajayan, *Nature chemistry* **2009**, *1*, 403.

[16] R. Kabiri, H. Namazi, *Journal of nanoparticle research* **2014**, *16*, 2474.

[17] T. E. Motaung, A. S. Luyt, F. Bondioli, M. Messori, M. L. Saladino, A. Spinella, G. Nasillo, E. Caponetti, *Polymer Degradation and Stability* **2012**, *97*, 1325-1333.

[18] M. Balci, *Basic 1H-and 13C-NMR spectroscopy*, Elsevier, **2005**.

[19] S. Stankovich, D. A. Dikin, R. D. Piner, K. A. Kohlhaas, A. Kleinhammes, Y. Jia, Y. Wu, S. T. Nguyen, R. S. Ruoff, *carbon* **2007**, *45*, 1558-1565.

[20] A. G. Shard, *Surface and Interface Analysis* **2014**, *46*, 175-185.